Environmental DNA

WILEY

Environmental DNA
Open Access
Dedicated to the study and use of environmental DNA for basic and applied sciences

ORIGINAL ARTICLE OPEN ACCESS

Interactions and Community Structure of Fungi and Prokaryotes in Salt and Brackish Marsh Ecosystems

Madeleine A. Thompson | Xuefeng Peng

School of Earth, Ocean, and Environment, University of South Carolina, Columbia, South Carolina, USA

Correspondence: Madeleine A. Thompson (mthompson@seoe.sc.edu) | Xuefeng Peng (xpeng@seoe.sc.edu)

Received: 14 February 2025 | **Revised:** 22 August 2025 | **Accepted:** 23 September 2025

Funding: This work was supported by the US NSF Division Of Environmental Biology (DEB) (DEB-2303089) and a University of South Carolina Advanced Support for Innovative Research Excellence (ASPIRE) grant awarded to Xuefeng Peng.

Keywords: estuarine microbiome | fungal-prokaryotic interactions | marine fungi | microbial interactions | network analysis

ABSTRACT

Microbial communities play a fundamental role in biogeochemical cycling within salt and brackish marsh ecosystems, yet fungal-prokaryotic interactions in these environments remain poorly understood. This study employed metabarcoding of the 16S and 28S rRNA genes to investigate prokaryotic and fungal communities across four locations in sediments and surface waters of the North Inlet salt marsh and Winyah Bay brackish marsh (South Carolina, USA) over four time points from 2020 to 2021. Co-occurrence network analyses were used to identify potential microbial interactions and their ecological implications. Distinct fungal and prokaryotic communities were observed between the two marsh types. From the 16S prokaryotic primer set, Proteobacteria, Bacteroidota, and Cyanobacteriota dominated both marshes. Early diverging fungi and Actinomycetota (bacteria) were prevalent in the brackish marsh, whereas salt marsh communities were primarily composed of Dikarya fungi (Ascomycota and Basidiomycota) and Desulfobacteria. Network analyses revealed contrasting interactions between surface water and sediment. In brackish marsh sediments, fungi and prokaryotes exhibited nearly exclusively negative connections, suggesting strong resource competition. In contrast, Dikarya fungi in brackish marsh surface water displayed numerous positive connections with bacteria, suggesting potential cross-feeding interactions. In the salt marsh, fungi and prokaryotes exhibited potential cooperative and competitive/antagonistic interactions. Ascomycota were positively connected with Desulfobacteria, suggesting a role in complex organic matter degradation. Conversely, negative connections between Chytridiomycota (early diverging fungi) and Cyanobacteriota (bacteria) implied parasitic interactions. These findings highlight the dynamic nature of fungal-prokaryotic interactions in coastal ecosystems. By analyzing potential microbial relationships in salt and brackish marshes, this study provides new insights into the ecological roles of fungi in estuarine environments, particularly their contributions to nutrient cycling and organic matter decomposition. Understanding these interactions is crucial for generating hypotheses and predicting microbial responses to environmental changes—such as shifts in salinity and nutrient availability—and their potential impacts on marsh ecosystem functioning.

1 | Introduction

Salt marshes are vital ecosystems that contribute to the ecological health and stability of coastal environments, serving as biodiversity hotspots that support a wide range of plant and animal species, including critical habitats for juvenile fish and other marine life (Simas et al. 2001; Barbier et al. 2011). These ecosystems act as natural buffers against storm surges, flooding, and erosion by absorbing wave energy and protecting inland areas from damage (Simas et al. 2001; Braatz et al. 2007; Shepard et al. 2011).

Additionally, salt marshes play a significant role in carbon sequestration, capturing and storing atmospheric carbon dioxide in their biomass and sediments, with estimates suggesting that between 4.8 and 87.2 Tg of carbon per year are sequestered in salt marsh sediments (Mcleod et al. 2011). Microbial communities within these marshes are essential for nutrient cycling and exhibit resilience to environmental stressors such as salinity and temperature variations (Crain 2007; Deegan et al. 2007; Czapla et al. 2020; Zhang et al. 2024). Understanding the dynamics of these microbial communities is critical for assessing the overall health and functionality of salt marsh ecosystems.

The interactions among microbial communities in salt marshes—including fungi and prokaryotes—are fundamental to ecosystem processes such as nutrient cycling and organic matter decomposition (Blum and Mills 2012; Kearns et al. 2019; Li, Cui, et al. 2022; Crump and Bowen 2024). These interactions can be competitive/antagonistic, including direct resource competition, production of inhibitory compounds, and parasitism (Amend et al. 2019; Peng et al. 2024; Wang and Kuzyakov 2024). In estuarine ecosystems, bacteria and fungi can compete strongly for limited resources, such as organic carbon, dissolved nutrients, and metabolic niches (Amend et al. 2019; Buesing and Gessner 2006; Peng et al. 2024; Wang and Kuzyakov 2024). Interference mechanisms, such as the production of antagonistic enzymes and secondary metabolites that inhibit microbial competitors, also play a large role in competitive interactions between bacteria and fungi (Amend et al. 2019; Buesing and Gessner 2006; Peng et al. 2024; Wang and Kuzyakov 2024). Some fungi secrete hydrolytic enzymes that degrade bacterial cell walls, while certain bacteria produce antibiotics or siderophores to suppress fungal growth (Wohl and McArthur 2001; Amend et al. 2019; Wang and Kuzyakov 2024). Parasitic interactions further influence antagonistic microbial dynamics, as fungal parasites such as Chytridiomycota target Cyanobacteriota, altering microbial community structure and nutrient fluxes (Gerphagnon et al. 2019; Gleason et al. 2014; Rasconi et al. 2009; Sime-Ngando 2012). These competitive and antagonistic interactions contribute to the regulation of microbial populations, preventing dominance by any single group and maintaining functional diversity within the ecosystem (Wang and Kuzyakov 2024).

Interactions between fungi and prokaryotes can also be cooperative, as fungi and prokaryotes engage in cross-feeding, co-metabolism, and nutrient exchange. These cooperative interactions facilitate organic matter degradation, drive nutrient cycling, and enhance microbial resilience in fluctuating environmental conditions (Li et al. 2015; van der Heijden et al. 2016; Amend et al. 2019; Wang and Kuzyakov 2024). Cross-feeding, where metabolic byproducts from one organism serve as substrates for another, plays a key role in fungal-bacterial cooperation (Wang and Kuzyakov 2024). Cross-feeding can enhance organic matter decomposition, promoting nutrient recycling and overall ecosystem stability (Wang and Kuzyakov 2024). Fungal extracellular enzymes can also initiate the breakdown of recalcitrant organic matter, while bacterial enzymes can complete the process, facilitating efficient decomposition (Bärlocher and Boddy 2016; de Menezes et al. 2017; Amend et al. 2019; Wang and Kuzyakov 2024). In addition to organic matter degradation, fungi and bacteria engage in nutrient exchange, such as ammonium introduced into nitrogen-limited environments through nitrogen fixation (Kaneko et al. 2002; Bedmar et al. 2005), stabilizing microbial communities and enhancing resilience (Griffiths and Philippot 2013; Toor et al. 2024).

Despite increasing interest in marine fungi, our understanding of their diversity, ecological roles, and interactions in coastal ecosystems remains limited. Recent environmental sequencing data, specifically using 28S rRNA gene primer sets (Picard 2017; Thompson et al. 2025), have revealed early diverging fungal lineages in estuarine ecosystems, such as Blastocladiomycota, Zoopagomycota, and Chytridiomycota, but their specific contributions to nutrient cycling are still poorly understood (Jones 2011; Comeau et al. 2016; Picard 2017; Duan et al. 2018; Pham et al. 2021; Thompson et al. 2025). Early diverging fungi have been understudied in coastal marshes compared to Dikarya fungi, which include well-known groups such as Ascomycota and Basidiomycota (Amend et al. 2019). This gap is significant because early diverging lineages, such as Blastocladiomycota, Zoopagomycota, and Chytridiomycota, represent some of the most ancient fungal groups, often exhibiting distinct life histories, morphologies, and ecological strategies (Myers et al. 2020; Wang et al. 2023). Their divergence from Dikarya suggests they may play unique and previously unrecognized roles in ecosystem processes, particularly in nutrient cycling and microbial interactions.

This study aims to analyze the potential interactions between fungi and prokaryotes in marsh ecosystems. By employing metabarcoding to investigate the prokaryotic 16S small subunit (SSU) and fungal 28S large subunit (LSU) rRNA regions and co-occurrence network analyses, we seek to enhance our understanding of how these microbial communities may interact in the North Inlet–Winyah Bay (NI–WB) estuary in South Carolina, USA. Our research examines both positive and negative connections between prokaryotes and fungi, highlighting their complex relationships. We hypothesize that environmental factors, such as salinity and sample type (sediment or surface water), influence these connections by exerting selective pressures on microbial community composition and diversity. Understanding the potential cooperation and competition/antagonism between prokaryotes and fungi is critical not only for advancing basic ecological theory but also for informing ecosystem management and conservation. Microbial communities underpin key biogeochemical processes, such as carbon and nitrogen cycling, that affect marsh productivity, water quality, and resilience to climate change (Leadbeater et al. 2021). Insights into microbial network structure and environmental drivers can help identify sensitive or keystone taxa, predict ecosystem responses to environmental disturbances, and guide restoration strategies (Zhou et al. 2010; Deng et al. 2012; Xiao et al. 2022). Ultimately, this work lays a foundation for integrating microbial ecology into coastal management and climate adaptation frameworks.

2 | Materials and Methods

2.1 | Study Area and Sample Collection

North Inlet–Winyah Bay (NI–WB), situated in Georgetown, South Carolina, USA, is a National Oceanic and Atmospheric

Administration (NOAA) National Estuarine Research Reserve (NERR), which includes four long-term monitoring sites: Oyster Landing, Clambank, Debidue Creek, and Thousand Acre (Figure 1; Allen et al. 2014). This NERR encompasses roughly 19,000 acres of tidal marshes with varying salinity levels. Winyah Bay is a brackish, river-dominated estuary influenced by the Waccamaw, Sampit, Black, and Pee Dee Rivers, with an average salinity of 7.5 ± 10.4, and it receives approximately 557 m^3/s of freshwater input annually (Patchineelam et al. 1999). The Thousand Acre monitoring station is positioned alongside Winyah Bay. The other three sampling sites—Clambank, Oyster Landing, and Debidue Creek—are located in different areas of the North Inlet estuarine system, which is a relatively pristine, high-salinity, ocean-dominated salt marsh with an average salinity of 29.6 ± 5.9 (Li, Wang, et al. 2022).

In June 2020, August 2020, February 2021, and November 2021, seawater and sediment samples (48 of each) were collected from NI–WB to investigate the seasonal diversity of fungi and prokaryotes across the brackish and salt marsh at four sites: Oyster Landing, Clambank, Debidue Creek, and Thousand Acre (Figure 1). The NERR monitored physical and chemical parameters at each location, including temperature, salinity, pH, and chlorophyll *a*. All samples were collected on the same day as the long-term monitoring nutrient samples, which included measurements of nitrate, nitrite, ammonium, and phosphate. Surface sediment samples were collected into sterile 1.5 mL tubes, and approximately 50 mL of surface water samples were filtered using a 0.22 μm Sterivex filter (EMD Millipore #SVGP01050, Burlington, MA). At each site, three biological replicates were collected during every sampling event. The samples were transported to the laboratory in a cooler and stored at −80°C until extraction.

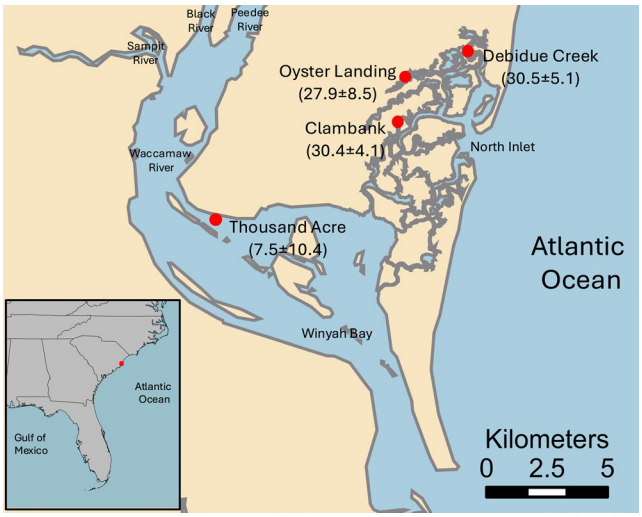

FIGURE 1 | Map of the study area (North Inlet–Winyah Bay, South Carolina, USA). The four sampling sites are marked by red circles and the average salinity ± standard deviation (measured using the Practical Salinity Scale (PSS-78)) from 2020 to 2021 at each site are included in parentheses below the site name. This figure was adapted from the University of Maryland Integration and Application Network (ian.umces.edu/media-library).

2.2 | DNA Extraction

In the laboratory, DNA was extracted from sediment samples using the DNeasy PowerSoil Pro Kit (Qiagen, Cat # 47014; DNeasy PowerSoil Pro Kit 2023), with a slight modification to the first step (cell lysis). Approximately 0.5 ± 0.01 g of sediment was weighed into MN bead tubes type A (Macherey-Nagel #740786.50) and bead-beaten in a Biospec Mini-BeadBeater-16 for 60 s. The remaining steps were performed according to the DNeasy PowerSoil Pro Kit protocol without further modifications. For DNA extraction from the Sterivex filters, the DNeasy PowerWater Kit was used, again modifying only the cell lysis step. Half of each Sterivex filter paper was cut into 2 mm squares using sterilized scissors and placed into MN bead tubes type A (Macherey-Nagel #740786.50). These were bead-beaten in a Biospec Mini-BeadBeater-16 for 60 s. All other extraction steps followed the DNeasy PowerWater Kit protocol without further modifications. DNA concentration was measured using a Qubit fluorometer, and samples were stored at −20°C until they were ready for amplification.

Following Illumina's 16S library protocol (Illumina #15044223Rev.B; Peng and Valentine 2021), we used a two-step PCR process: the first step involved amplicon PCR, and the second step consisted of Index PCR. For sequencing the V4–V5 regions of the 16S and 18S rRNA genes, the universal primer set 515F-Y (5′-GTGYCAGCMGCCGCGGTAA-3′) and 926R (5′-CCGYCAATTYMTTTRAGTTT-3′) was used (Parada et al. 2015). To sequence the 28S LSU region of fungi, the primer set LR0R (5′-ACSCGCTGAACTTAAGC-3′) and LF402 (5′-TTCCCTTTYARCAATTTCAC-3′) was used (Tedersoo et al. 2015).

Each sample went through a 10 μL PCR reaction protocol in triplicates, with the following mixture: 0.1 μL of forward primer, 0.1 μL of reverse primer, 2 μL of 5× GC Buffer (Thermo Scientific #F530S, Vilnius, LT), 0.2 μL of 10 mM dNTPs (Thermo Scientific #R0181, Vilnius, LT), and 0.1 μL of Phusion High-Fidelity DNA Polymerase (Thermo Scientific #F530S, Vilnius, LT). The thermal cycling conditions for the universal primer set began with an initial denaturation at 98°C for 30 s, followed by 25 cycles of denaturation at 98°C for 10 s, annealing at 50°C for 30 s, and extension at 72°C for 45 s, concluding with a final elongation at 72°C for 10 min. For the 28S primer set, the cycling conditions included an initial denaturation at 98°C for 30 s, followed by 30 cycles of 98°C for 10 s, 53°C for 30 s, and 72°C for 45 s, ending with a final elongation at 72°C for 10 min.

The triplicates were pooled and cleaned using sparQ PureMag beads at a 1:1 ratio of beads to PCR products, following the sparQ PureMag bead cleanup protocol (Quantabio #95196/IFU-124.1 REV 03) without modifications. The cleaned PCR products were quantified using the High Sensitivity 1× DNA Qubit. Unique indices were assigned to each sample prior to sequencing, utilizing the Nextera XT DNA Library Preparation Kit (Illumina #FC-131-1096). The indexed amplicon libraries underwent a second round of cleaning using the same bead cleanup protocol. In total, 293 amplicon libraries were pooled to achieve a concentration of 2 nM and sent to the Duke Genome Center for sequencing in one lane of an 2 × 250 bp paired-end (PE) on a

NovaSeq 6000 SP flow cell on the Illumina NovaSeq 6000 platform, generating raw reads from 16S and 28S libraries.

2.3 | Sequence Analysis

For 16S sequencing reads, raw reads were quality filtered using bbduk.sh (Bushnell et al. 2017) with the following parameters: ktrim = *r*, ordered, minlen = 51, minlenfraction = 0.33, mink = 11, tbo, tpe, rcomp = f, k = 23, hdist = 1, hdist2 = 1, ftm = 5, pigz = t, unpigz = t, zl = 4, and ow = true. These parameters were selected to maximize read retention while removing low-quality bases and adapter contamination. Specifically, ktrim = *r* trims adapters from the right end, minlen and minlenfraction ensure only sufficiently long reads are kept, and hdist values allow for minimal mismatches in k-mer matching to improve accuracy. This step was followed by Trimmomatic (Bolger et al. 2014) with the parameters: ILLUMINACLIP:$adapters:2:30:10, LEADING:3, TRAILING:3, SLIDINGWINDOW:4:15, and MINLEN:200 to further trim poor-quality leading/trailing bases and apply a dynamic sliding window filter, ensuring only high-confidence reads were retained for downstream analysis. The filtered forward and reverse reads were then merged using USEARCH v11.0.667 (Edgar 2010) with the "-fastq_mergepairs" function. Merged reads were quality filtered with a maximum expected error (maxEE) set to 2 using the "-fastq_filter" function, which balances read quality and data retention. The reads were dereplicated using the "-fastx_unique" function and clustered into 10,130 operational taxonomic units (OTUs) at 97% similarity with the "-cluster_otus" function (Dataset S1) (Thompson et al. 2025). The nucleotide sequences of the 16S OTUs were imported to QIIME2 v2023-5 (Caporaso et al. 2010) and classified by a Naïve Bayesian Classifier using the SILVA v138.1–99 as the reference database (Quast et al. 2012). The 18S sequencing reads obtained from the universal primer set had identified only three fungal OTUs (Thompson et al. 2025), so the 18S reads were not used in further analyses.

A previous study found that the 28S rRNA gene primer set targeting the D1 region using the RDP database identified a broader and more taxonomically rich marine fungal community, including many early diverging fungi, in salt and brackish marsh surface waters and sediments, compared to the commonly used ITS2 primer set (Thompson et al. 2025). For the 28S sequencing reads, raw reads were quality filtered using bbduk.sh (Bushnell et al. 2017) with the following parameters: ktrim = *r*, ordered, minlen = 51, minlenfraction = 0.33, mink = 11, tbo, tpe, rcomp = f, k = 23, hdist = 1, hdist2 = 1, ftm = 5, pigz = t, unpigz = t, zl = 4, and ow = true, as well as Trimmomatic (Bolger et al. 2014) with the parameters: ILLUMINACLIP:$adapters:2:30:10, LEADING:3, TRAILING:3, SLIDINGWINDOW:4:15, and MINLEN:200. The filtered forward and reverse reads were then merged using USEARCH v11.0.667 (Edgar 2010) with the "-fastq_mergepairs" function and filtered with a maximum expected error (maxEE) set to 1 using the "-fastq_filter" function. The reads were dereplicated using the "-fastx_unique" function and clustered into 8461 operational taxonomic units (OTUs) at 97% similarity with the "-cluster_otus" function (Dataset S1) (Thompson et al. 2025). The nucleotide sequences of the 28S primer OTUs were classified using the RDP classifier version 2.14 (Wang et al. 2007; Wang and Cole 2024).

2.4 | Statistical and Network Analyses

2.4.1 | Community Composition Analysis

The relative abundance of each 16S OTU was calculated via the phyloseq package in R (McMurdie and Holmes 2013). Taxa that included groups that had a maximum relative abundance of < 1% across all samples were grouped together and labeled as "Other". A list of these "Other" phyla and their average relative abundance can be found in Dataset S6. Stacked bar charts and other analyses for the 28S OTUs are described in Thompson et al. (2025). Using the vegan package in R, a pairwise PERMANOVA (permutations = 999) was completed to determine the significance of the 16S diversity between the marsh sampling locations. *p*-values were adjusted using Benjamini-Hochberg (*p*.adjust function in R stats package method = "BH") for multiple comparisons. Environmental parameters of the surface water, including nutrients (such as nitrate, nitrite, phosphate, and ammonium), dissolved oxygen, salinity, temperature, pH, and chlorophyll *a* content at each station on the day of sampling, were investigated via weighted unifrac principal coordinates analysis (PCoA) to determine prokaryotic roles in shaping the microbial community composition in the surface water via the ape package in R. A PERMANOVA (vegan package in R) for PCoA was conducted to determine the significance of the environmental variables.

2.4.2 | Co-Occurrence Network Analyses

Microbial co-occurrence networks have become an essential tool in microbial ecology, providing insights into potential interactions within microbial communities and serving as a foundation for hypothesis generation (Banerjee et al. 2018; Röttjers and Faust 2018). Numerous tools have been widely adopted for constructing these networks, including SparCC (Friedman and Alm 2012), SpiecEasi (Kurtz et al. 2015), MENAP (Deng et al. 2012), and WGCNA (Langfelder and Horvath 2008). For our analysis, we chose the Molecular Ecological Network Analyses Pipeline (MENAP) due to its robustness against noise and recent enhancement with the iDIRECT module, which effectively identifies indirect interactions within networks (Xiao et al. 2022).

Network analyses of the 28S fungal communities and 16S prokaryotic communities at two sample locations (Clambank and Thousand Acre) and type (sediment and surface water) were performed using the Molecular Ecological Network Analyses Pipeline (MENAP) (Zhou et al. 2010, 2011; Deng et al. 2012; Xiao et al. 2022). Pairwise PERMANOVA analysis comparing the surface water prokaryotic communities showed that the prokaryotic communities were not significantly different between the salt marsh sites (Dataset S1). Pairwise PERMANOVA analysis comparing the sediment prokaryotic communities showed that the R^2 values were consistently higher when comparing one of the salt marsh sites against the brackish site (0.50, 0.51, 0.50; Table S2) than when comparing among the salt marsh sites (0.15,

0.13, 0.12; Table S2). Therefore, one salt marsh site and the brackish site were selected for network analysis. The OTU abundance table per primer set for each station and sample type was rarefied to the same sequencing depth (Table S3) (Cameron et al. 2021). Unequal sequencing depth was observed across the dataset, and rarefaction was performed to ensure comparability of microbial co-occurrence patterns across groups. The rarefied 16S and 28S OTU tables for each station and sample type were merged. The 16S/28S rarefied OTU table was used to construct the network using the random matrix theory-based network approach (Chavda et al. 2014). To construct robust and interpretable networks, only OTUs observed in 100% of samples within a given site and type (e.g., Clambank sediment, Clambank surface water, Thousand Acre sediment, Thousand Acre surface water) were included in the respective network. The relative abundance of OTUs was transformed using a centered log-ratio and a Pearson correlation coefficient (Zhou et al. 2010). A chi-squared test on Poisson distribution was used to determine the correlation and significance. Within MENAP, positive relationships are defined as statistically significant positive correlations ($r > 0$), indicating potential co-occurrence or cooperative interactions, while negative relationships are defined as significant negative correlations ($r < 0$), suggesting mutual exclusion or potential competition/antagonism. Network global properties, individual nodes' centrality, and module separation and modularity calculations (greedy modularity optimization) were calculated as part of the MENAP pipeline. The completed network was visualized in Cytoscape v3.9.1 (Shannon et al. 2003). Putative keystone OTUs were identified using the criteria $P_i < 0.6$ and $Z_i > 1.5$. Z_i indicates how well a node is connected to other nodes in the same module. P_i indicates how well a node is connected to different modules, calculated using equations from (Guimerà and Amaral 2005; Xiao et al. 2022). The MENAP used included a recently added module, iDIRECT, which removes indirect connections between nodes by eliminating self-looping and the values of the total interaction strengths outside their natural range (Xiao et al. 2022).

2.4.3 | Potential Functional Predictions for Fungi and Prokaryotes

FUNGuild (Nguyen et al. 2016) was used to analyze the functional guilds of fungi in ecological communities (Dataset S1) by searching the genus name identified by RDP in the FUNGuild database. PICRUSt2 (Douglas et al. 2020) was used to predict the functional potential of prokaryotic microbial communities based on the taxonomic composition (Dataset S2–S5), using the picrust2_pipeline.py function in the PICRUSt2 bioinformatics software package. Additional functional descriptions to those predictions were added using the add_descriptions.py function with the "-m KO" (KEGG Orthology IDs were mapped to functional names) (Douglas et al. 2020).

3 | Results

3.1 | Environmental Context

Salinity levels (measured using the Practical Salinity Scale [PSS-78]) varied across sites, with Clambank, Oyster Landing, and Debidue Creek in North Inlet having an average salinity of 30.4, 27.9, and 30.5, respectively (range of 6.5–41.6), compared to Thousand Acre in Winyah Bay, where salinity averaged 7.5 and ranged from 0.1 – 26.7 (Thompson et al. 2025; Figure 2). Salinity in Clambank, Oyster Landing, and Debidue Creek peaked in November 2020 and was the lowest in March 2021 (Figure 2). Salinity in Thousand Acre peaked in November 2021 (Figure 2). Chlorophyll *a* levels peaked at Clambank, Oyster Landing, and Debidue Creek during the summer months, with the highest values recorded in May 2020 (77.1 $\mu g L^{-1}$) and July 2021 (22.2 $\mu g L^{-1}$) at Clambank (Figure 2). Thousand Acre showed much higher peaks, reaching 172.1 $\mu g L^{-1}$ in August 2020 and 96.9 $\mu g L^{-1}$ in July 2021 (Figure 2). Nitrate (NO_3^-; 0.04–4.8 μM) and nitrite (NO_2^-; 0.05–0.2 μM) levels were consistently low at Clambank, Debidue Creek, and Oyster Landing (Figure 2). Thousand Acre had more fluctuation, reaching a nitrate concentration of 0.5 μM during February 2021 and a nitrite concentration of 0.01 μM during August 2021 (Figure 2). Ammonium (NH_4^+) concentrations fluctuated between 0.0 and 0.25 μM at Clambank, Debidue Creek, and Oyster Landing, while Thousand Acre peaked at 0.3 μM during August 2021 (Figure 2). Phosphate (PO_4^{3-}) concentrations fluctuated between 0.0 and 0.05 μM at Clambank, Debidue Creek, and Oyster Landing, while Thousand Acre peaked at 0.09 μM during January 2020 (Figure 2).

3.2 | Prokaryotic Community Composition and Diversity

A total of 10,130 prokaryotic OTUs (clustered at 97% similarity) were identified using the chosen 16S primer set. Across sediment samples from both sites, Proteobacteria consistently dominated the prokaryotic community, accounting for an average of 34.4% across all seasons (Figure 3). Within this phylum, Gammaproteobacteria and Alphaproteobacteria were the most abundant subphyla, particularly during the winter months (February and November 2021), comprising 41.2% and 16.0% of the sediment community, respectively. Other dominant phyla in the sediment included Cyanobacteriota (16.3%), Bacteroidota (12.1%), and Desulfobacteria (9.2%) (Figure 3). Desulfobacteria were more abundant in salt marsh sediment (6.2% on average) than in brackish marsh sediment (2.6% on average). Bacteroidota were found in sediment and surface water samples but were more abundant in surface water (27.2% on average) than in sediment (12.1% on average). Bacteroidota peaked in sediment during February 2021, reaching 38.4% of the prokaryotic community composition (Figure 3). In surface water samples, Cyanobacteriota exhibited seasonal variation, with higher relative abundance in summer months (27.7% on average in June and August 2020) and a decline in winter (14.4% on average) (Figure 3). In Thousand Acre surface water, Actinomycetota and Acidobacteriota peaked in November 2021 at 9.9% and 2.3%, respectively (Figure 3). Unclassified prokaryotic taxa accounted for a small fraction of the total prokaryotic community, averaging 0.4% of reads (Figure 3). Thermoproteati (TACK [Thaumarchaeota, Aigarchaeota, Crenarchaeota, and Korarchaeota] group) had a low relative abundance across all samples (0.01%), but reached a relative abundance of 1.5% in June 2020 in salt marsh surface water samples (Figure 3).

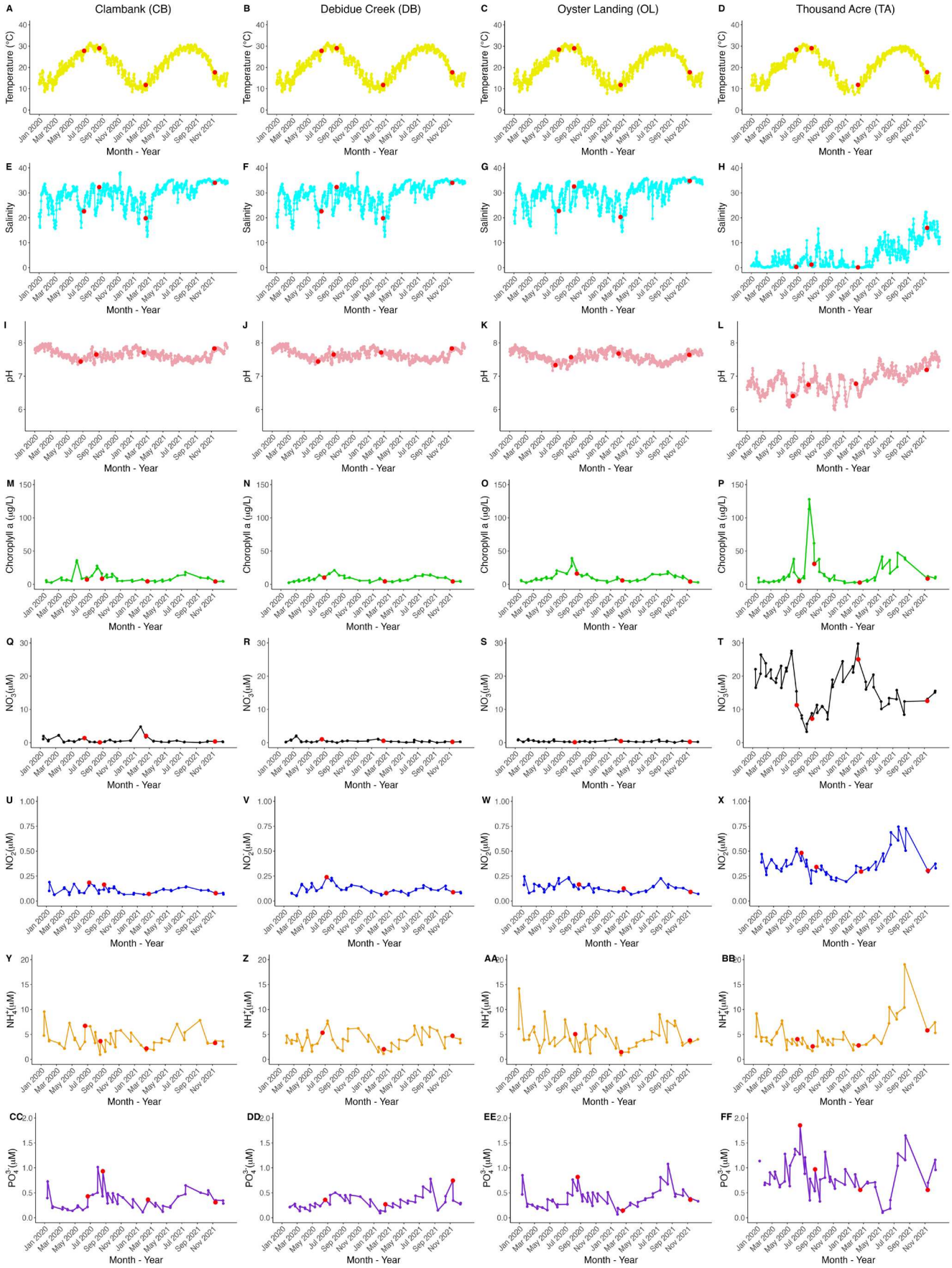

FIGURE 2 | Legend on next page.

FIGURE 2 | Surface water temperature (yellow; A–D), salinity (blue; E–H), pH (pink; I–L), chlorophyll a (green; M–P), nitrate (Q-T), nitrite (U–X), ammonium (Y-BB), and phosphate (CC-FF) measurements from Clambank (A, E, I, M, Q, U, Y, CC), Debidue Creek (B, F, J, N, R, V, Z, DD), Oyster Landing (C, G, K, O, S, W, AA, EE), and Thousand Acre (D, H, L, P, T, X, BB, FF) from January 2020 to January 2022. The red dots indicate the sampling dates. Data were collected via the National Estuarine Research Reserve's long-term monitoring program.

There were significant differences in prokaryotic community composition between salinity ranges in both sediment and surface water (Figure 4; Table S2), as well as the fungal community composition (Thompson et al. 2025). Prokaryotic communities differed significantly between Thousand Acre and salt marsh sampling locations (pairwise PERMANOVA, $p < 0.005$, Table S2). There were strong differences in sediment communities among several sampling locations, with the largest differences observed between Clambank and Thousand Acre ($R^2 = 0.50$, $p = 0.0015$) and between both of these sites and Debidue Creek or Oyster Landing (all $p < 0.005$; Table S2). Nutrients, such as phosphate, nitrate, and nitrite, significantly influenced prokaryotic community structure, explaining 1.9%, 2.5%, and 4.7% of the total variation, respectively (PERMANOVA, $p < 0.01$). Other significant factors included temperature ($R^2 = 4.6\%$), pH ($R^2 = 8.9\%$), and sampling date ($R^2 = 1.8\%$) (all $p < 0.01$, Table S4). Sampling station and sample type (sediment vs. surface water) also accounted for significant variation in community composition ($R^2 = 2.1\%$, $p < 0.01$).

3.3 | Fungal Community Composition and Diversity

A total of 3624 fungal OTUs were identified from the 28S rRNA primer set, revealing significant differences in fungal communities between salt and brackish marshes (Thompson et al. 2025). In salt marsh sediments, Ascomycota were consistently the dominant fungal phylum, making up an average of 80.0% of the community (Figure 5). The sediment samples were primarily composed of various Sordariomycetes (Thompson et al. 2025), while surface water samples were dominated by Capnodiales and Pleosporales, two orders within Dothideomycetes (Thompson et al. 2025). In the brackish marsh, although Ascomycota remained the most prevalent phylum, its relative abundance was notably lower, averaging 37.9%. Instead, Zoopagomycota and Chytridiomycota made up significant portions of the fungal community, averaging 23.8% and 21.5%, respectively (Figure 5). Zoopagomycota, primarily represented by Entomophthorales (Thompson et al. 2025), were more abundant during summer 2020 than in winter 2021, peaking at 52.3% relative abundance in Thousand Acre surface water in August 2020. Chytridiomycota were commonly found across samples, with average relative abundances of 14.1% in sediment and 9.4% in surface water (Figure 5). Blastocladiomycota, largely from the Catenariaceae family (Thompson et al. 2025), were especially common in the water column of the brackish marsh, with a peak relative abundance of 10.4% and an overall average of 3.1% (Figure 5). Mucoromycota were also detected but remained at low abundance, averaging just 1.1% (Figure 5).

3.4 | Co-Occurrence Network Analyses

3.4.1 | Interactions in Salt Marsh Sediment

The 16S/28S co-occurrence network for Clambank sediment (281 nodes, 400 connections) revealed a complex microbial structure dominated by prokaryotes such as Gammaproteobacteria (19.6% of nodes), Bacteroidota (15.3%), Planctomycetota (12.1%), Actinomycetota (7.1%), and Desulfobacteria (6.4%), and fungi such as Ascomycota (10.6%) (Figure 6). Eighteen bacterial and six fungal keystone OTUs ($Z_i > 1.5$, $P_i < 0.6$) were identified (Figure 6; Table S5). Gammaproteobacteria, especially from Steroidobacterales, Sedimenticolaceae (keystone species from Chromatiales order), and *Ketobacter* (keystone species from Oceanospirillales order), exhibited both negative (Steroidobacterales; No. 135 in Figure 6, Sedimenticolaceae; No. 167 in Figure 6; Table S5) and positive (*Ketobacter*; No. 149 in Figure 6; Table S5) interactions with Ascomycota (Figure 6; Dataset S7). Cellvibrionales (Gammaproteobacteria) showed mixed interactions, with negative links predominating (negative connections: No. 152, 160 in Figure 6; positive connections: No. 248 in Figure 6) (Table S6; Dataset S7). Within Ascomycota, *Aspergillus* (keystone species from Eurotiomycetes class; No. 60 in Figure 6; Table S5) formed mostly positive connections with Rhizobiales (Alphaproteobacteria; No. 63 in Figure 6), *Phaeoacremonium* (keystone species from Sordariomycetes class; No. 43 in Figure 6; Table S5), *Trichoderma* (keystone species from Sordariomycetes class; No. 44 in Figure 6; Table S5), and other Sordariomycetes (No. 46, 55, 57, 58, 194 in Figure 6) formed mostly positive connections with Desulfobulbales (Desulfobacteria; No. 168, 170, 183 in Figure 6) and negative links with Rhizobiales (Alphaproteobacteria; No. 63 in Figure 6), Bacteroidota (Bacteroidales; No. 39 in Figure 6, and Ignavibacteriales; No. 25 in Figure 6), and Actinomycetota (Microtrichales; No. 78, 79, 91, 199 in Figure 6; and Solirubrobacterales No. 90 in Figure 6), and Dothideomycetes (No. 52, 54, 56 in Figure 6) had positive connections to Cytophagales (Bacteroidota; No. 37 in Figure 6) and negative interactions with Phycisphaerales (Planctomycetota; No. 120 in Figure 6) and Phycisphaeraceae (keystone species from Phycisphaerales order; No. 122 in Figure 6; Table S5) (Figure 6; Table S6; Dataset S7).

Other fungi, including Blastocladiomycota, Chytridiomycota, and Zoopagomycota, displayed unique interaction patterns: *Catenomyces* (keystone species from Blastocladiomycota phylum; No. 9 in Figure 6; Table S5) and *Coelomomyces* (Blastocladiomycota; No. 8 in Figure 6) were negatively associated with HOC36 (Gammaproteobacteria; No. 151 in Figure 6) but positively with Ascomycota (No. 47) and Desulfobulbales (Desulfobacteria; No. 177 in Figure 6), while Chytridiomycota

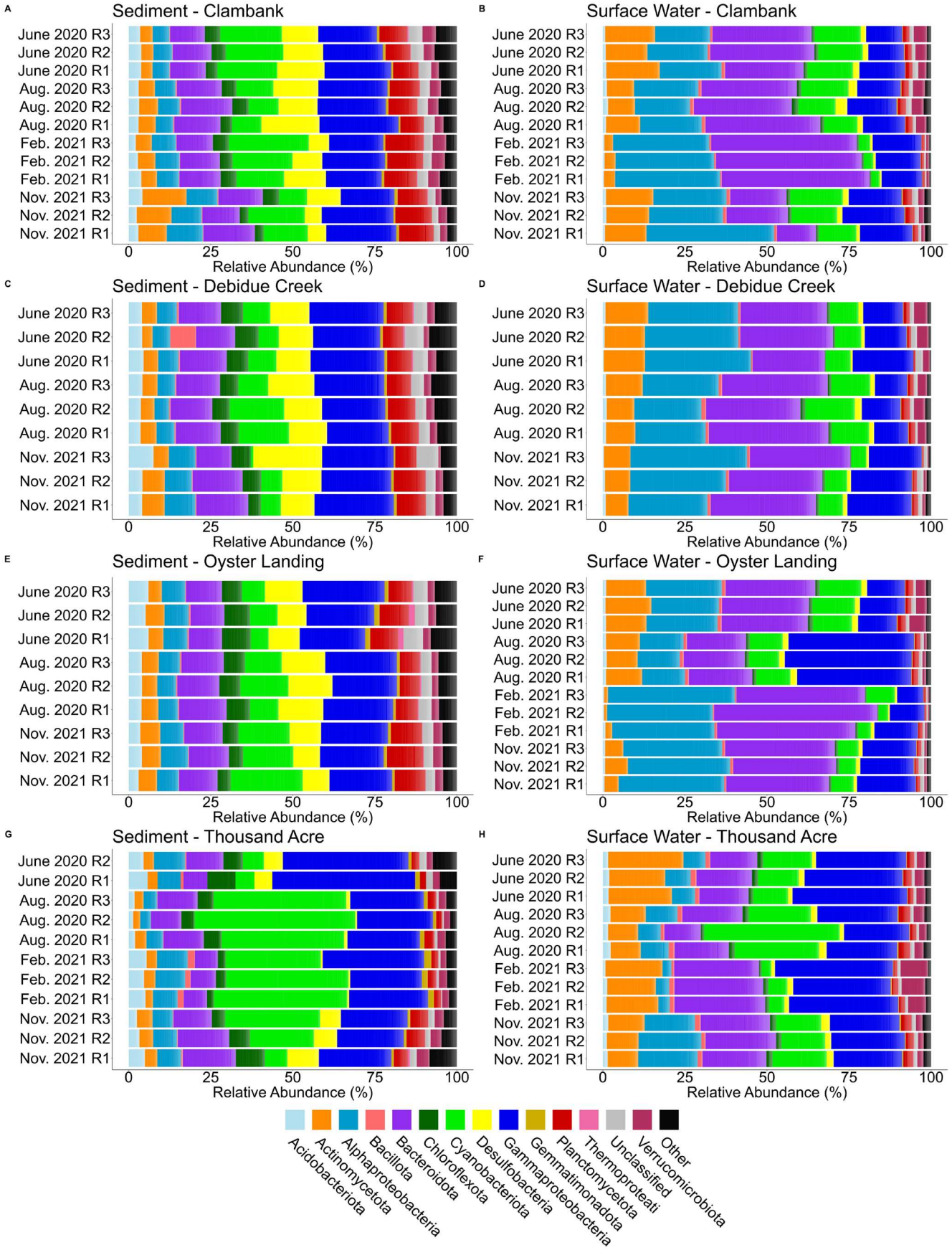

FIGURE 3 | Legend on next page.

FIGURE 3 | Relative abundance of 16S OTUs across all sampling dates (June 2020, August 2020, February 2021, and November 2021) in: (A) sediment, Clambank; (B) surface water, Clambank; (C) sediment, Debidue Creek; (D) surface water, Debidue Creek; (E) sediment, Oyster Landing; (F) surface water, Oyster Landing; (G) sediment, Thousand Acre; and (H) surface water, Thousand Acre. Data are shown for biological replicates R1, R2, and R3. Bars are colored by OTU taxonomic assignment at the phylum or class level. Taxa with a maximum relative abundance < 1% across all samples were grouped as "Other," with their average and maximum abundances provided in Dataset S6. Bacillota corresponds to the phylum previously named Firmicutes.

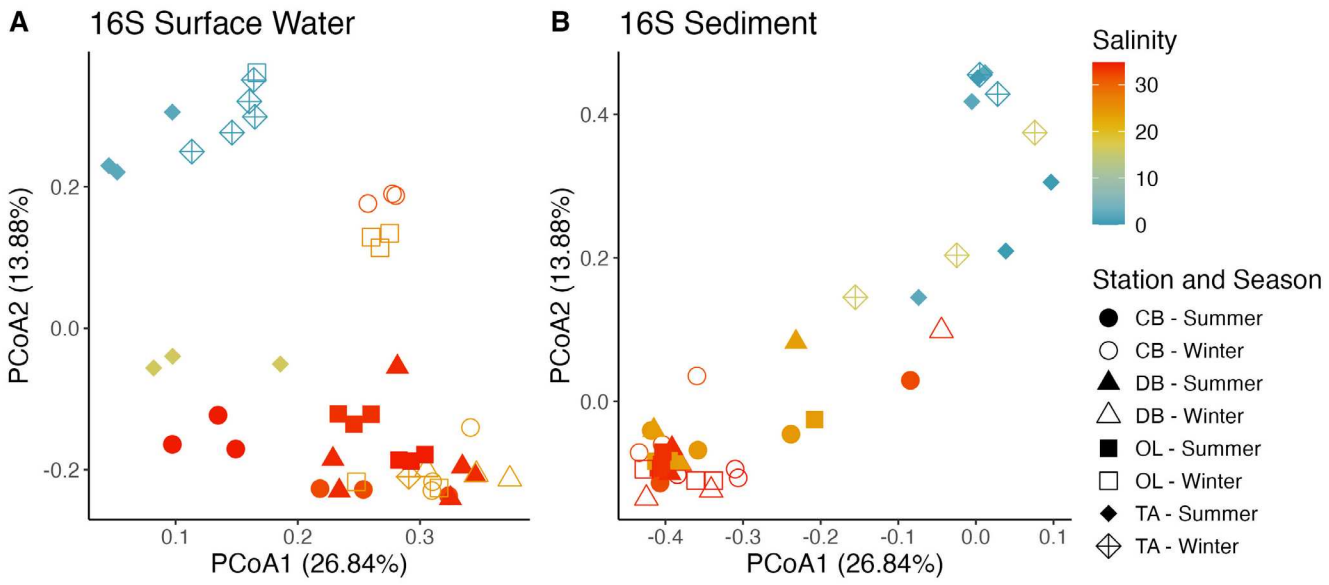

FIGURE 4 | Weighted UniFrac principal coordinate analysis (PCoA) ordinations based on 16S 97% OTUs from all four study sites—Clambank (CB), Debidue Creek (DB), Oyster Landing (OL), and Thousand Acre (TA). Samples are shown for (A) surface water and (B) sediment. Shapes indicate sampling location, shaded symbols represent summer (June and August), and open symbols represent winter (February and November). Points are colored by the average salinity (from 2020 to 2021).

(No. 191, 192, and 193 in Figure 6) had positive interactions with Rhodobacterales (Alphaproteobacteria; No. 67 in Figure 6) and Desulfobacterales (Desulfobacteria; No. 179 in Figure 6) but negative ones with Leptolyngbyales (Cyanobacteria; No. 189 in Figure 6) and OM190 (Planctomycetota; No. 124 in Figure 6; Table S6; Dataset S7). Zoopagomycota (No. 97 and 236 in Figure 6) had both positive (with MSBL9 (Planctomycetota; No. 237 in Figure 6)) and negative (with Rhodobacterales (Alphaproteobacteria; No. 75 in Figure 6)) associations (Figure 6; Table S6; Dataset S7). The network suggests a highly connected community with functional diversity, where key taxa like Gammaproteobacteria and Ascomycota influence community structure.

3.4.2 | Interactions in Salt Marsh Surface Water

The Clambank surface water network (362 nodes, 1932 connections) was dominated by Bacteroidota (27.1%), Gammaproteobacteria (26.2%), and Alphaproteobacteria (12.4%), with 17 bacterial and one fungal keystone OTU identified (Figure 7; Table S7). Ascomycota formed positive and negative connections with Bacteroidota, Gammaproteobacteria, and Alphaproteobacteria (Figure 7). Within Bacteroidota, Ascomycota (No. 61, 63, 64, 65, 66 in Figure 7) had positive interactions with Flavobacteriales (No. 49, 51, 57, 227 in Figure 7) but negative ones with Chitinophagales (No. 6, 220 in Figure 7), Cytophagales (No. 43, 225 in Figure 7), and Bacteroidales (No. 56 in Figure 7; Table S8). Within Gammaproteobacteria, Ascomycota (No. 63, 66 in Figure 7) showed positive associations with B2M28 (No. 152 in Figure 7) but negative connections with Cellvibrionales (No. 144 in Figure 7; Table S8). Oceanospirillales (No. 136, 257 in Figure 7), Comamonadaceae (keystone species from Burkholderiales order; No. 134 in Figure 7; Table S7), and other Burkholderiales (No. 135, 139, 143, 147 in Figure 7) formed both positive and negative connections with Ascomycota (No. 61, 63, 66, 258 in Figure 7; Table S8). Among Alphaproteobacteria, Ascomycota (No. 61, 62, 63, 65, 66 in Figure 7) had mixed connections with Rhizobiales (No. 72, 77 in Figure 7), *Planktomarina* (keystone species from Rhodobacterales order; No. 74 in Figure 7; Table S7), and other Rhodobacterales (No. 67, 76, 79, 80 in Figure 7; Table S8). Ascomycota (No. 63, 66 in Figure 7) also formed positive associations with Actinomycetota (Frankiales; No. 104, 107 in Figure 7), Planctomycetota (No. 120, 121 in Figure 7), and Desulfobacteria (No. 195, 196 in Figure 7). Latescibacterota (No. 325 in Figure 7) had only negative connections with Ascomycota (No. 326 in Figure 7; Table S8). The network reflects a dynamic microbial ecosystem, where cooperative and antagonistic relationships coexist, shaping community structure.

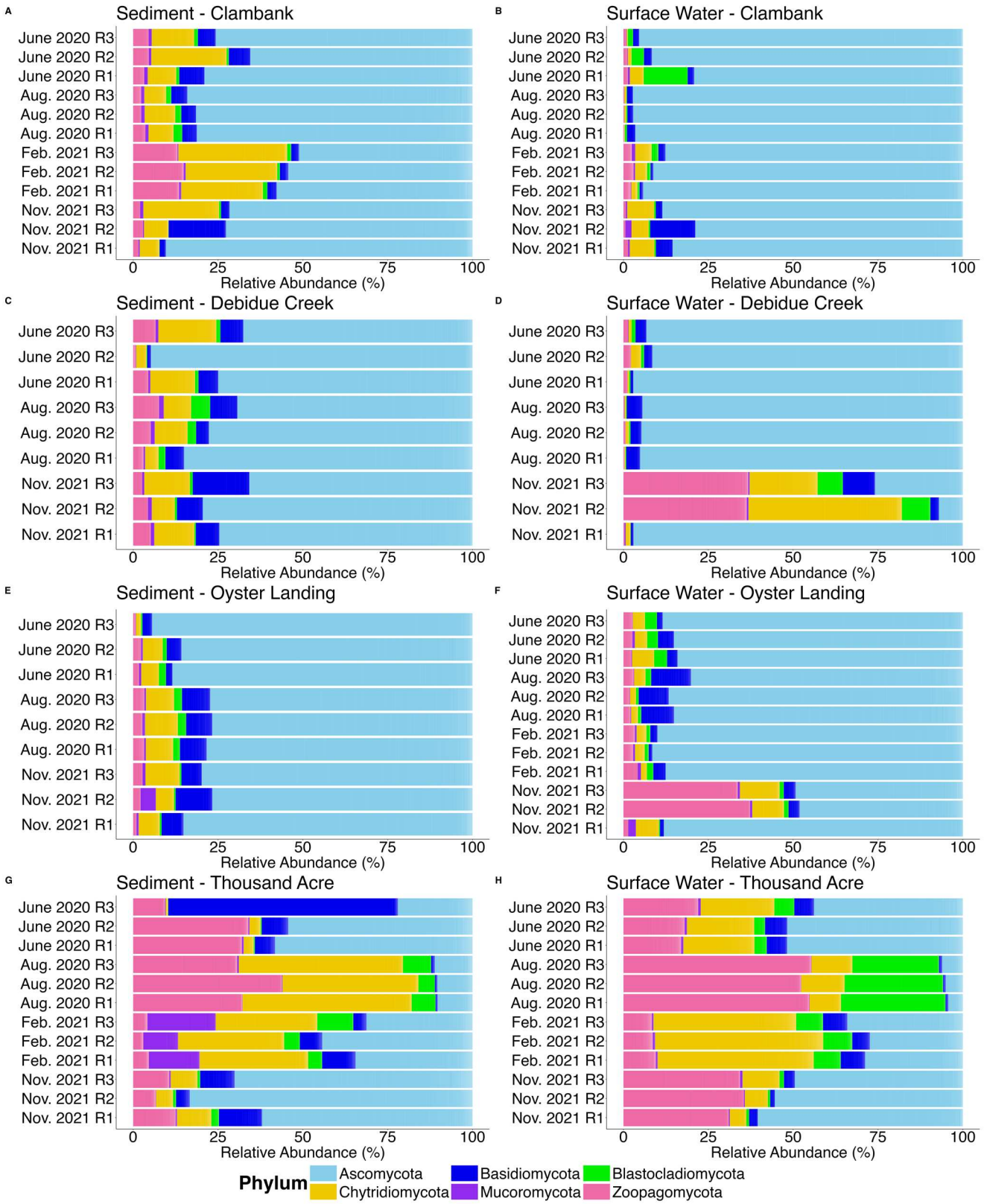

FIGURE 5 | Relative abundance of 28S OTUs across all sampling dates (June 2020, August 2020, February 2021, and November 2021) in: (A) sediment, Clambank; (B) surface water, Clambank; (C) sediment, Debidue Creek; (D) surface water, Debidue Creek; (E) sediment, Oyster Landing; (F) surface water, Oyster Landing; (G) sediment, Thousand Acre; and (H) surface water, Thousand Acre. Data are shown for biological replicates R1, R2, and R3. Bars are colored by OTU taxonomic assignment at the phylum level.

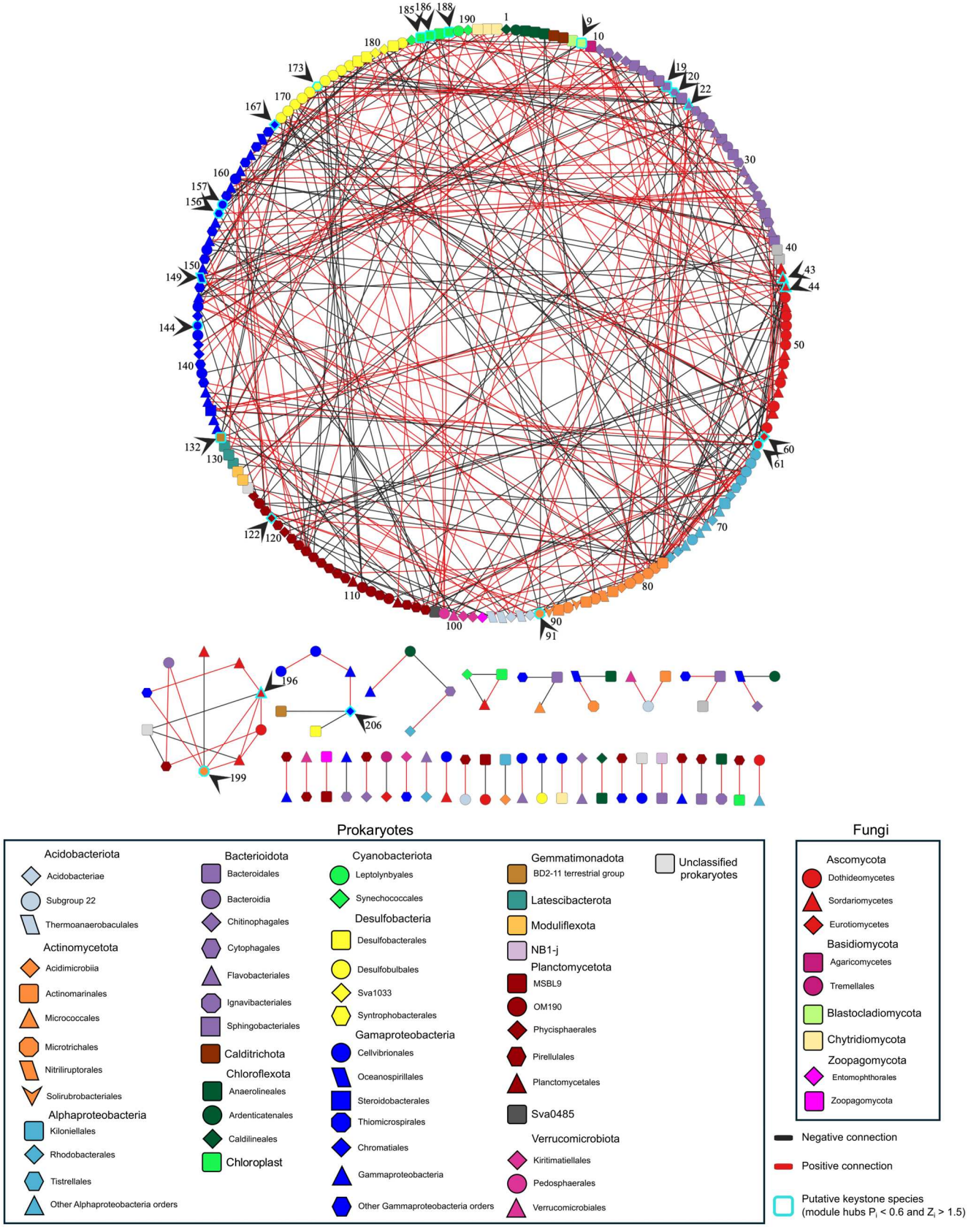

FIGURE 6 | Co-occurrence network of fungi (28S) and prokaryotes (16S) in Clambank sediment. Positive connections are shown in red and negative connections in black. Nodes are colored by phylum (with Alphaproteobacteria and Gammaproteobacteria shown separately), and node shapes represent prokaryotic order or fungal class. A teal outline and black arrow highlight OTUs identified as putative keystone taxa ($Z_i > 1.5$ and $P_i < 0.6$). An interactive version of the network is available at: https://www.ndexbio.org/#/network/d68a197d-72e4-11f0-a218-005056ae3c32?accesskey=e0fb5bcbed96c77b4165c95aa40f0d090120df98e1fda5f34f431790966034f4.

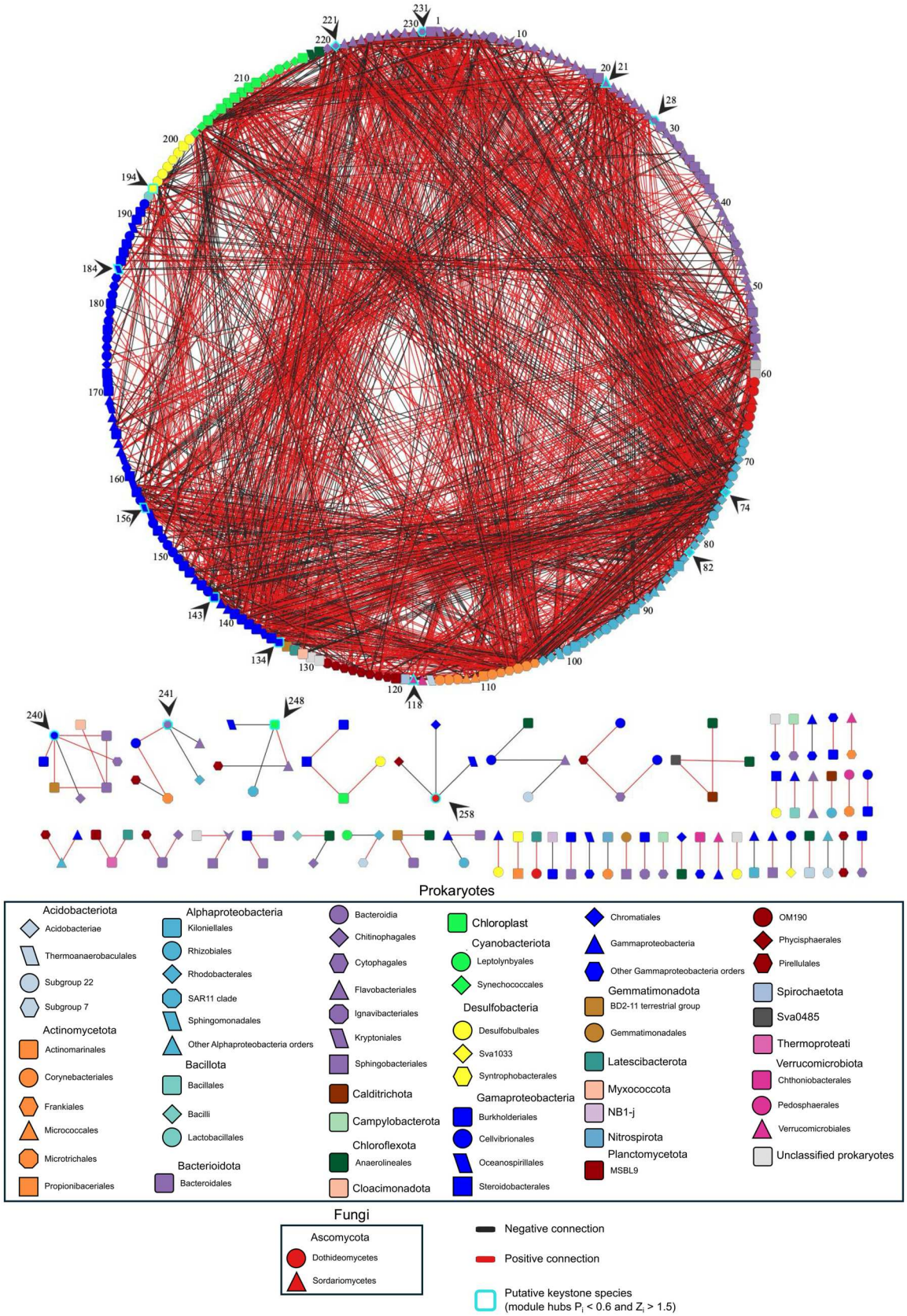

FIGURE 7 | Co-occurrence network of fungi (28S) and prokaryotes (16S) in Clambank surface water. Positive connections are shown in red and negative connections in black. Nodes are colored by phylum (with Alphaproteobacteria and Gammaproteobacteria shown separately), and node shapes represent prokaryotic order or fungal class. A teal outline and black arrow highlight OTUs identified as putative keystone taxa ($Z_i > 1.5$ and $P_i < 0.6$). An interactive version of the network is available at: https://www.ndexbio.org/#/network/68cb4884-72e7-11f0-a218-005056ae3c32?accesskey=5e4ebf179efc3acd088443437d012a57d46636ecc5f0b9125e65df48697912ba.

3.4.3 | Interactions in Brackish Marsh Sediment

The Thousand Acre sediment network (123 nodes, 247 connections) was dominated by Ascomycota (36.6%), Gammaproteobacteria (22.7%), and Bacteroidota (5.7%). Eight bacterial and one fungal keystone OTU were identified (Figure 8; Table S9). Dothideomycetes (No. 7, 10, 12, 13, 15, 21, 22, 26, 29, 32, 34, 40, 108 in Figure 8; one keystone OTU (*Microdiplodia*; No. 34 in Figure 8; Table S9), Eurotiomycetes (No. 6, 24, 36), Sordariomycetes (No. 5, 8, 9, 11, 20, 25, 27, 37, 38, 117, 123 in Figure 8), and other Ascomycota classes (No. 19 in Figure 8) formed exclusively negative interactions with Acidobacteriota (subgroup 17; No. 51, 52, 53 in Figure 8), Actinomycetota (Microtrichales; No. 46, 49 in Figure 8), Bacteroidota (Cytophagales; No. 3, 104, 105 in Figure 8), *PHOS-HE36* (keystone species from Ignavibacteriales order; No. 1 in Figure 8; Table S9), and other Ignavibacteriales; No. 2 in Figure 8), Chloroflexi (*UTCFX1* (keystone species from Anaerolineales order; No. 99 in Figure 8; Table S9), *Aerolinea* (keystone species from Anaerolineales order; No. 101 in Figure 8; Table S9), and other Anaerolineales; No. 98, 100 in Figure 8), Chloroplast (No. 96, 97 in Figure 8), Desulfobacteria (Desulfobacterales; No. 95 in Figure 8 and Desulfobulbales; No. 92 in Figure 8), Gemmatimonadota (Gemmatimonadales; No. 63, 64 in Figure 8), Planctomycetota (Planctomycetales; No. 59 in Figure 8), Verrucomicrobiota (Verrucomicrobiales; No. 57 in Figure 8), and Gammaproteobacteria (Cellvibrionales; No. 66 in Figure 8, Comamonadaceae (keystone species from Burkholderiales order; No. 69, 89, 90 in Figure 8; Table S9), Burkholderiales; No. 67, 71, 72, 73, 79, 85, 86, 87, 88 in Figure 8, B2M28; No. 83 in Figure 8, and Chromatiales; No. 84), suggesting antagonism or competition (Figure 8; Table S10). In contrast, Ascomycota (No. 13, 14, 15, 16, 17, 18, 19, 21, 22, 25, 26, 27, 28, 29, 30, 31, 32, 33, 34, 35, 36, 37, 39, 40, 113, 114, 115, 118, 119 in Figure 8) had positive interactions with other fungal groups within Ascomycota (No. 14, 15, 16, 17, 18, 19, 21, 22, 25, 26, 27, 28, 29, 30, 31, 32, 33, 34, 35, 36, 39, 40, 113, 114, 115, 118, 119 in Figure 8), Zoopagomycota (No. 56 in Figure 8), and Basidiomycota (No. 103 in Figure 8) (Table S10).

Basidiomycota (No. 102, 103 in Figure 8) had negative interactions with *Lapillicoccus* (keystone species from Micrococcales order; No. 47 in Figure 8; Table S9), Chloroplast (No. 96 in Figure 8), Comamonadaceae (keystone species from Burkholderiales order; No. 69 in Figure 8; Table S9), and other Burkholderiales (No. 70, 71, 89 in Figure 8) but a positive one with Sordariomycetes (No. 37 in Figure 8) (Table S10). Zoopagomycota (No. 55, 56, 120 in Figure 8) showed negative connections with Desulfobacterales (Desulfobacteria; No. 91 in Figure 8) and Cytophagales (Bacteroidota; No. 105 in Figure 8) but a positive one with Chytridiomycota (No. 121 in Figure 8) and Dothideomycetes (No. 13 in Figure 8) (Table S10). The network suggests high competition and cooperation within the microbial community, with Ascomycota as a central player in microbial dynamics.

3.4.4 | Interactions in Brackish Marsh Surface Water

The Thousand Acre surface water network (222 nodes, 1153 connections) was primarily composed of Gammaproteobacteria (22.5%), Bacteroidota (20.2%), Actinomycetota (13.8%), and Ascomycota (9.4%). Fourteen bacterial keystone OTUs were identified, but no fungal keystone OTUs were detected (Figure 9; Table S11). Ascomycota (No. 18, 19, 20, 21, 22, 23, 24, 25, 26, 27, 28, 29, 167 in Figure 9) exhibited both positive and negative connections with *TRA3-20* (keystone species from Burkholderiales order; No. 114 in Figure 9; Table S11), Comamonadaceae (keystone species from Burkholderiales order; No. 116 in Figure 9; Table S11), and other Burkholderiales (No. 96, 97, 98, 99, 104, 109, 110, 111, 112, 113, 117,120, 123, 134 in Figure 9), Chitinophagales (No. 158, 162, 166 in Figure 9), *NS11-12 marine group* (keystone species from Sphingobacteriales order; No. 155 in Figure 9; Table S11; and No. 154 in Figure 9), with most being positive (Figure 9; Table S12; Dataset S10). Other bacterial groups, including Sporichthyaceae (keystone species from Frankiales order; No. 53, 55, 57 in Figure 9; Table S11), Cytophagales (No. 160 in Figure 9), Micrococcales (No. 59, 60, 62 in Figure 9), Myxococcota (No. 95 in Figure 9), Rhizobiales (No. 34, 35, 37, 52 in Figure 9), Rickettsiales (No. 169 in Figure 9), Verrucomicrobiae (No. 87, 88, 89 in Figure 9), and fungal groups like Ascomycota (No. 21, 23, 25, 27, 28 in Figure 9), Zoopagomycota (No. 85 in Figure 9), and Basidiomycota (No. 148 in Figure 9), were also positively connected to Ascomycota (No. 17, 18, 19, 20, 21, 23, 24, 25, 27, 28, 29, 167 in Figure 9), indicating cooperative relationships (Figure 9; Table S12; Dataset S10). However, negative connections with Ascomycota (No. 18, 19, 20, 23, 29, 210 in Figure 9) were observed with Cellvibrionales (No. 105 in Figure 9), Fluviicola (keystone species from Flavobacteriales order; No. 149 in Figure 9; Table S11), and other Flavobacteriales (No. 153, 156, 157, 161, 209 in Figure 9), Rhodobacterales (No. 30 in Figure 9), Chloroflexi (No. 144 in Figure 9), and Pirellulales (No. 93 in Figure 9). Basidiomycota (No. 148, 180 in Figure 9) had negative connections with Phycisphaerales (No. 179 in Figure 9) but positive ones with Comamonadaceae (No. 116 in Figure 9; Table S11) and Dothideomycetes (No. 21, 24 in Figure 9) (Table S12; Dataset S10).

Chytridiomycota (No. 143 in Figure 9) displayed negative connections with SAR11 clade (No. 32 in Figure 9) and positive ones with Flavobacteriales (No. 159 in Figure 9). Zoopagomycota (No. 85 in Figure 9) displayed positive connections with Actinomycetota (No. 78, 60 in Figure 9), Myxococcota (No. 95 in Figure 9), and Burkholderiales (No. 117, 116 in Figure 9), indicating complex interdependencies (Figure 9; Table S12; Dataset S10). Overall, the network reflects a highly interconnected microbial community with mutualistic and antagonistic relationships shaping its structure.

3.4.5 | Functional Potential of Prokaryotic Microbial Communities

The potential functional roles of prokaryotic taxa varied between sites and sample types (Figure 10). Adenylyl-sulfate reductase (EC 1.8.99.2), associated with dissimilatory sulfur metabolism, was represented primarily by orders within the phylum Desulfobacteria, including Desulfobacterales, Desulfobulbales, and Desulfatiglandales. In sediments, Clambank (CB) showed a higher predicted functional abundance of adenylyl-sulfate reductase from Desulfobacterales, Desulfobulbales, and Desulfatiglandales than Thousand Acre (TA) sediments. In

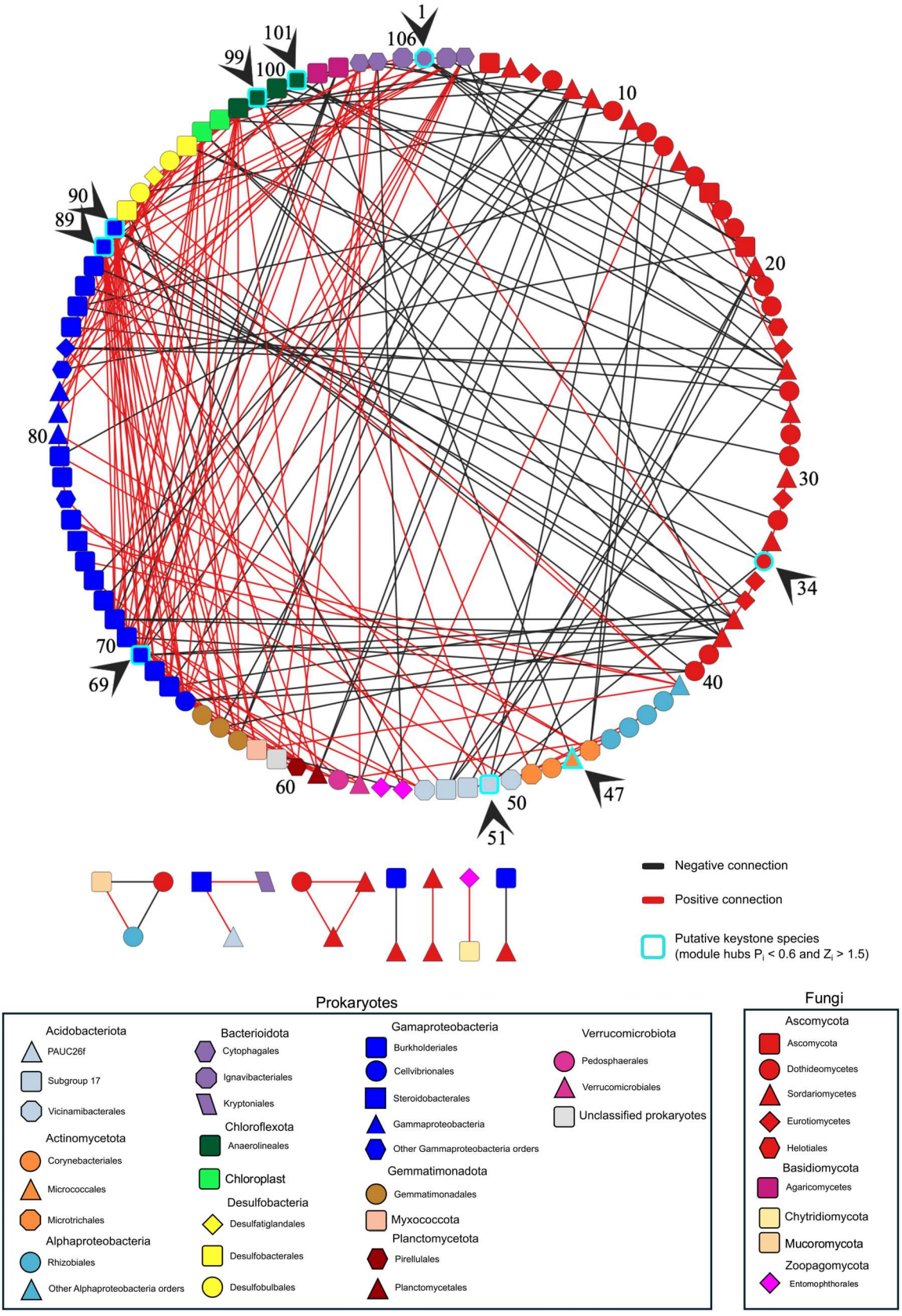

FIGURE 8 | Co-occurrence network of fungi (28S) and prokaryotes (16S) in Thousand Acre sediment. Positive connections are shown in red and negative connections in black. Nodes are colored by phylum (with Alphaproteobacteria and Gammaproteobacteria shown separately), and node shapes represent prokaryotic order or fungal class. A teal outline and black arrow highlight OTUs identified as putative keystone taxa ($Z_i > 1.5$ and $P_i < 0.6$). An interactive version of the network is available at: https://www.ndexbio.org/#/network/640730c1-72e7-11f0-a218-005056ae3c32?accesskey=14b8236ecf344bb4bfb047790fcc6b948574e6fbbcbe7142d52f8aae0cd07539.

surface waters, the predicted functional abundance of adenylylsulfate reductase was similar between CB and TA.

Beta-glucosidase (EC 3.2.1.21) was found across multiple phyla. In sediments, CB beta-glucosidase predicted functional abundance was higher in Bacteroidales (Bacteroidota), Cytophagales (Bacteroidota), Flavobacteriales (Bacteroidota), and Rhodobacterales (Alphaproteobacteria) than in the TA sediment, while TA sediment had a higher predicted functional abundance of beta-glucosidase in Burkholderiales (Alphaproteobacteria) and Chitinophagales (Bacteroidota) than in CB sediment (Figure 10). CB surface waters had high predicted functional abundance for beta-glucosidase from Flavobacteriales (Bacteroidota), Rhodobacterales (Alphaproteobacteria), and Oceanospirillales (Gammaproteobacteria). In TA surface waters, Chitinophagales (Bacteroidota), Cytophagales (Bacteroidota), and Burkholderiales (Alphaproteobacteria) had a higher predicted functional abundance for beta-glucosidase than in the CB surface water (Figure 10).

Beta-lactamase (EC 3.5.2.6) was also distributed among several Bacteroidota and Gammaproteobacteria orders, with high predicted functional abundance in CB sediment for Bacteroidales and Flavobacteriales, and TA sediment enriched in Burkholderiales and Chitinophagales (Figure 10). In surface waters, predicted functional abundance was high for CB, dominated by Flavobacteriales. In TA surface water, predicted functional abundance was high for Burkholderiales and Chitinophagales, similarly to beta-glucosidase (Figure 10).

Cellulase (EC 3.2.1.4) was primarily associated with Actinomycetota, including Actinomarinales and Solirubrobacterales, both abundant in CB sediment, and Corynebacteriales abundant in TA sediment (Figure 10).

Nitrogenase (EC 1.18.6.1) was associated mainly with Rhizobiales (Alphaproteobacteria). In sediments and surface water, TA showed higher predicted functional abundance than CB (Figure 10).

The potential functional roles of fungi varied across sites and sample types (Figure 11). In sediments, saprotrophic groups—including those involved in litter, wood, and other organic matter decomposition—were the most abundant and showed the highest OTU richness compared to surface water (Figure 11A). TA sediment had elevated richness in litter and wood saprotrophs, foliar endophytes, and other decomposer roles, while CB sediment also showed high richness in saprotrophs along with fungi that are necrotrophic on roots and plant pathogens. In surface water, overall fungal richness was lower, with communities dominated almost entirely by saprotrophic roles, particularly litter and wood decomposition, and with higher richness in TA than CB (Figure 11B). Several functional groups found in sediments were absent from water samples. TA surface water also showed elevated richness in litter and wood saprotrophs. CB surface water had relatively higher richness in fungi that are necrotrophic on roots and wood/leaf/seed saprotrophs compared to TA (Figure 11B).

4 | Discussion

4.1 | Fungal and Prokaryotic Contributions in Estuarine Ecosystems

Fungi and prokaryotes are key drivers of biogeochemical processes in estuarine ecosystems, playing critical roles in nutrient cycling and organic matter decomposition (Blum and Mills 2012; Kearns et al. 2019; Li, Cui, et al. 2022; Crump and Bowen 2024). In NI–WB, prokaryotes support aerobic and anaerobic respiration, nitrogen fixation, denitrification, and sulfur cycling, while fungal guilds specialize in breaking down plant-derived and other recalcitrant substrates. Functional predictions from PICRUSt2 (Douglas et al. 2020) indicate strong site- and sample type-specific differences (Figure 10), with dominant phyla contributing to carbon, nitrogen, and sulfur transformations. These functional distributions paralleled the compositional patterns (Figure 3), where Proteobacteria, Cyanobacteriota, Bacteroidota, and Desulfobacteria were among the most abundant phyla and were consistent with the known metabolic versatility of these groups in marsh ecosystems (Dini-Andreote et al. 2014; Flood et al. 2015; Tebbe et al. 2022; Ge et al. 2025).

Proteobacteria were particularly dominant in NI–WB, with Gammaproteobacteria dominant in all samples and Alphaproteobacteria most abundant in the salt marsh surface water samples (Figure 3). Gammaproteobacteria specialize in breaking down polysaccharides and proteins, facilitating carbon cycling, and making organic compounds bioavailable to other organisms (Alonso-Sáez and Gasol 2007). Genera such as *Pseudomonas* (OTU2778, OTU9286, OTU148, OTU9836), known for denitrification (Carlson and Ingraham 1983; Jin et al. 2015), reached a relative abundance of up to 2.1% in sediment and 0.5% in surface water. In Alphaproteobacteria, *Bradyrhizobium*, a member of Rhizobiales and a known nitrogen fixer (Kaneko et al. 2002; Bedmar et al. 2005), complements the nitrogenase activity predicted for Rhizobiales in Figure 10, which may enhance bioavailable nitrogen in these marshes. *Bradyrhizobium* (OTU1059, OTU2761) reached up to 0.2% relative abundance in brackish marsh sediments. Other Alphaproteobacteria, such as Rhodobacterales and SAR11 clade, excel in metabolizing particulate organic carbon (Kong et al. 2021) and dissolved organic carbon (Alonso-Sáez and Gasol 2007; Denef et al. 2016; Sidhu et al. 2024), respectively. Rhodobacterales (OTU1565, OTU4, OTU29) also contributed to beta-glucosidase pathways (Figure 10), enabling the breakdown of plant-derived polysaccharides and other beta-D-glucoside-containing compounds into glucose (Ketudat Cairns and Esen 2010), which may support carbon turnover in both sediments and surface waters. Rhodobacterales accounted for 8.2% on average across all NI–WB samples and up to 30.4% in the salt marsh surface waters in February 2021 (Dataset S1). SAR11 clade accounted for 1.8% on average across all NI–WB samples and up to 28.6% of the microbial community in salt marsh surface waters in November 2021 (Figure S1) and is globally recognized for its dominance in nutrient-poor surface waters (Alonso-Sáez and Gasol 2007; Denef et al. 2016; Sidhu et al. 2024).

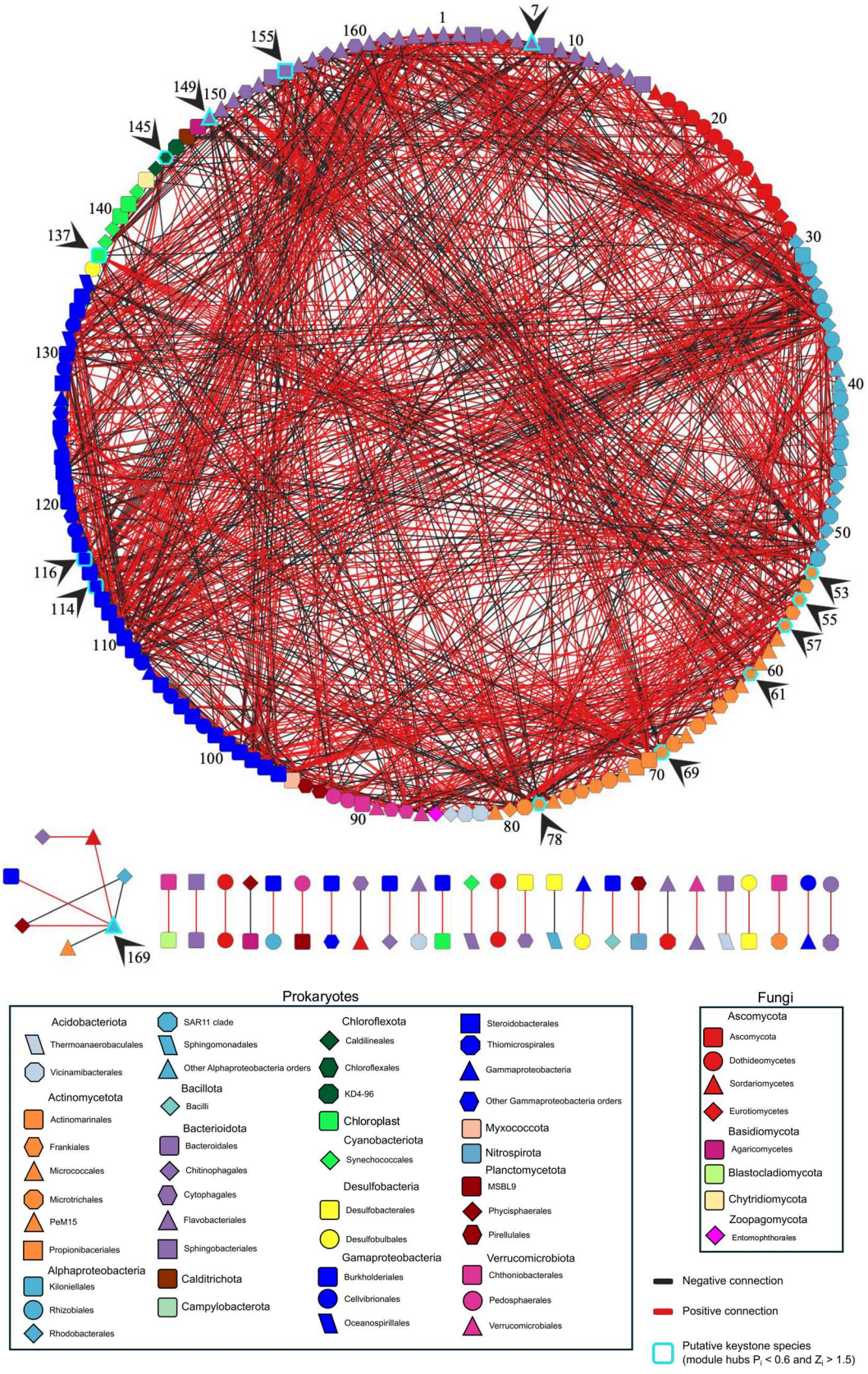

FIGURE 9 | Co-occurrence network of fungi (28S) and prokaryotes (16S) in Thousand Acre surface water. Positive connections are shown in red and negative connections in black. Nodes are colored by phylum (with Alphaproteobacteria and Gammaproteobacteria shown separately), and node shapes represent prokaryotic order or fungal class. A teal outline and black arrow highlight OTUs identified as putative keystone taxa ($Z_i > 1.5$ and $P_i < 0.6$). An interactive version of the network is available at: https://www.ndexbio.org/#/network/2a376706-73a4-11f0-a218-005056ae3c32?accesskey=8d27a599c84ed2a656a3fe0436747d80173bf94e245c143fd91dbb60e456c07e.

Other prokaryotic groups, including Actinomycetota, Cyanobacteriota, Bacteroidota, and Desulfobacteria, played significant roles in the NI–WB prokaryotic community (Figure 3). Cyanobacteriota were abundant in surface waters during summer, with their distribution likely driven by nutrient availability, temperature, and light (Figure 2). Brackish marsh conditions, characterized by elevated nitrate, ammonium, and phosphate, may have supported their high relative abundance (Murrell and Lores 2004; Carstensen et al. 2015), as reflected by peaks in chlorophyll *a* concentrations (Figure 2). Within Bacteroidota, orders such as Bacteroidales (OTU1900), Flavobacteriales (OTU124, OTU152, OTU5729, OTU709, OTU113), and Cytophagales (OTU42, OTU93, OTU1217, OTU32, OTU343, OTU5917) were linked to beta-lactamase and beta-glucosidase pathways (Figure 10), suggesting roles in both resisting microbial antagonism and degrading complex carbohydrates from marsh vegetation and phytoplankton. These orders are relatively abundant in the surface water (Figure S2). Desulfobacteria, more abundant in salt marsh sediments than in the brackish marsh (Figure 3; Figure S3), are sulfate-reducing bacteria that thrive in anoxic, sulfate-rich environments (Demin et al. 2024; Magnuson et al. 2023). They use enzymes such as dissimilatory adenylyl-sulfate reductase (Figure 10), which catalyzes the reduction of adenosine-5′-phosphosulfate to sulfite and adenosine monophosphate (Watanabe et al. 2016). This activity plays a central role in anaerobic organic matter degradation and can support methane oxidation when coupled with methanotrophic archaea in syntrophic partnerships (Bell et al. 2022; Qian et al. 2023), including associations with *Candidatus* Methanoperedens detected in NI–WB (OTU6140).

Fungi can complement these prokaryotic functions by breaking down recalcitrant organic matter through enzymatic processes (Bärlocher and Boddy 2016; de Menezes et al. 2017; Amend et al. 2019; Wang and Kuzyakov 2024). Ascomycota dominated organic matter decomposition (Figure 11; Figure S4), particularly in salt marsh samples (Figure 5), with FUNGuild assignments showing Sordariomycetes and Dothideomycetes as abundant litter and wood saprotrophs, foliar endophytes, and plant pathogens (Figure 11; Figure S4; Dataset S1). Litter and wood saprotrophs contribute to the breakdown of marsh plant detritus, accelerating carbon and nutrient release into sediments (Carrasco-Barea et al. 2022), while foliar endophytes may influence plant health and resilience under salt stress (Guo et al. 2023; Ameen et al. 2024). Many of these guilds likely express cellulase and related enzymes, enabling the hydrolysis of cellulose-rich vascular plant debris, which is a major component of high-marsh wrack and root material (Wang et al. 2016; Behera and Das 2023). Plant pathogen guilds identified within Sordariomycetes (Figure 11; Figure S4) could affect the turnover of dominant marsh vegetation, indirectly shaping detrital input to sediment microbial food webs. Basidiomycota contributed mainly to wood and soil decomposition (Figure 11; Figure S4; Dataset S1). In NI–WB, these guilds are likely important for decomposing coarse woody debris and lignified plant tissues, which are otherwise resistant to decay, thereby enhancing long-term carbon turnover (Boer et al. 2005). Early diverging fungal groups, dominant in the brackish marsh (Figure 5), such as Chytridiomycota and Blastocladiomycota, play dual roles as decomposers of particulate organic matter (POM) and parasites of plant and algal material (Figure 11; Figure S4; Dataset S1), influencing both primary production and nutrient recycling (Agha et al. 2016; Amend et al. 2019; Sen et al. 2022; Peng et al. 2024). Zoopagomycota were largely identified as saprotrophs (Figure 11; Figure S4; Dataset S1), contributing to the breakdown of organic debris and potentially recycling nutrients from decaying plant and algal material in marsh sediments and surface waters (Calabon et al. 2021).

4.2 | Putative Interactions Between Fungi and Prokaryotes in North Inlet–Winyah Bay

The co-occurrence network analyses for the salt and brackish marshes revealed intricate microbial interactions, highlighting both competitive and cooperative dynamics between fungi and prokaryotes (Figures 6–9). These interactions are crucial for shaping microbial community structure and driving biogeochemical processes. In this section, we emphasize the functional roles of specific taxa and their contributions to processes such as organic matter decomposition, nutrient cycling, and ecosystem stability.

4.3 | Resource Competition and Functional Overlap

In estuarine ecosystems, bacteria and fungi frequently compete for limited resources such as organic carbon, dissolved nutrients, and metabolic niches, shaping community structure and function (Amend et al. 2019; Buesing and Gessner 2006; Peng et al. 2024; Wang and Kuzyakov 2024). The co-occurrence network analysis revealed that Ascomycota (Dothideomycetes, Sordariomycetes, and Eurotiomycetes) exhibited negative interactions with several bacterial groups, including Desulfobacteria (Desulfobacterales and Desulfobulbales) in brackish marsh sediment (No. 92 and 95 in Figure 8), Bacteroidota (Ignavibacteriales, Cytophagales, and Bacteroidales) in most networks (No. 39 and 25 in Figure 6; No. 43, 225, and 56 in Figure 7; & No. 3, 104, 105, 1, and 2 in Figure 8), and Actinomycetota (*Ilumatobacter* (from Microtrichales order; No. 90, 91 in Figure 6), Microtrichales and Solirubrobacterales) in the salt and brackish marsh sediment networks (No. 78, 79, 199 in Figure 6; & No. 46, 49 in Figure 8), suggesting direct resource competition. Functional predictions indicate that Desulfobacterales and Desulfobulbales use dissimilatory adenylyl-sulfate reductase (Figure 10) to drive anaerobic sulfate reduction, potentially competing with fungal saprotrophs for the same organic carbon substrates in oxygen-limited sediments. Solirubrobacterales are linked to cellulase, while Cytophagales and Bacteroidales are linked to beta-glucosidase and beta-lactamase pathways (Figure 10), which parallel the lignocellulose-degrading capacities of Sordariomycetes and Dothideomycetes saprotroph guilds (Figure 11). This functional overlap suggests that bacteria and Ascomycota target similar plant-derived polysaccharides and other complex organic matter, intensifying competition in carbon-limited environments. Ascomycota had exclusively negative connections with bacterial groups in brackish marsh sediment, reinforcing the likelihood of broad-scale competition for detrital resources (Figure 8).

Zoopagomycota, largely identified as saprotrophs (Figure 11; Figure S4; Dataset S1), had negative connections with

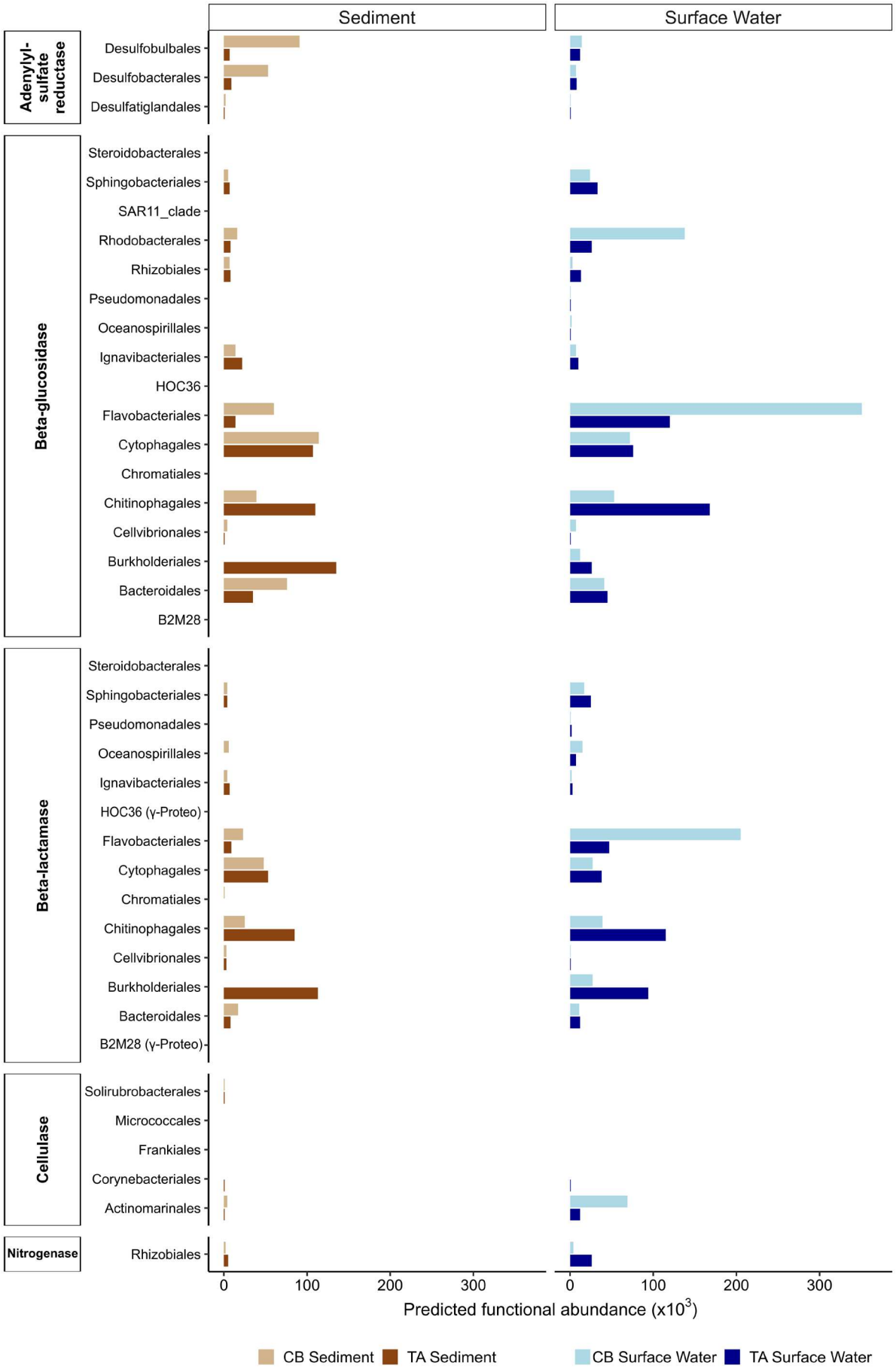

FIGURE 10 | Legend on next page.

FIGURE 10 | Potential functional roles and taxonomic orders of select prokaryotes identified using PICRUSt2 (Douglas et al. 2020). Bars represent the PICRUSt2-predicted functional abundance assigned to each select order across A) sediment and B) surface water samples from Clambank (CB) and Thousand Acre (TA) marshes in North Inlet–Winyah Bay. B2M28 and HOC36 are orders from Gammaproteobacteria. Bars representing Clambank are shown in lighter shades, while those representing Thousand Acre are shown in darker shades.

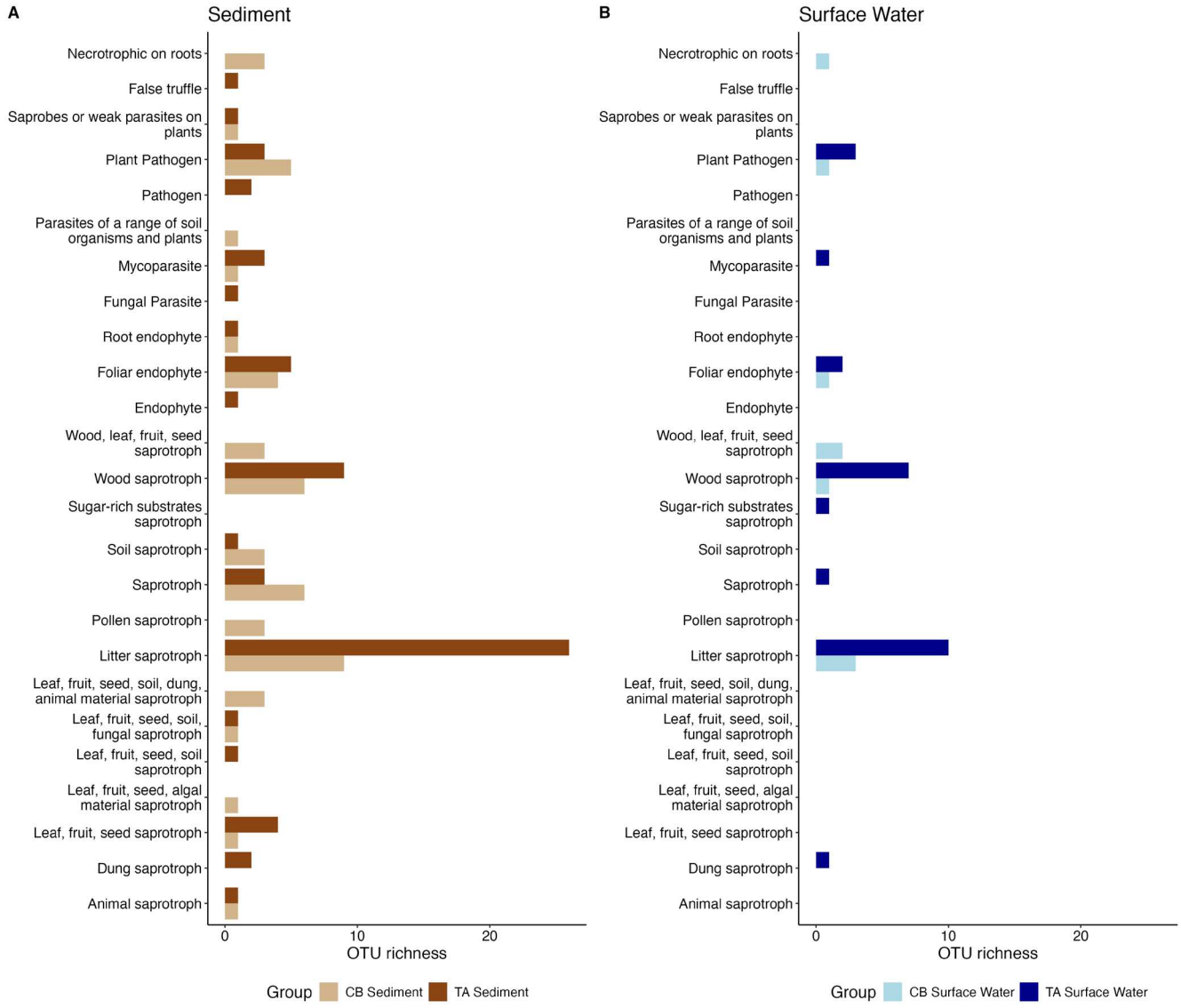

FIGURE 11 | Potential functional roles of fungal OTUs from the network analyses (Figures 6–9), identified using FUNGuild (Nguyen et al. 2016). Bars represent the number of unique OTUs assigned to each functional category in (A) sediment and (B) surface water samples from Clambank (CB) and Thousand Acre (TA) marshes in North Inlet–Winyah Bay. Bars representing Clambank are shown in lighter shades, while those representing Thousand Acre are shown in darker shades.

Rhodobacterales (Alphaproteobacteria) in the salt marsh sediment network (No. 75 in Figure 6) and with Desulfobacterales and Cytophagales in the brackish marsh sediment network (No. 91 and 105 in Figure 8). These bacterial groups are associated with beta-glucosidase and dissimilatory adenylyl-sulfate reductase (Figure 10), indicating potential competition with Zoopagomycota for access to dissolved and particulate organic matter pools derived from plant and algal detritus.

4.4 | Antagonistic Interactions and Chemical Interference

The production of inhibitory compounds also shapes microbial communities. Fungi and bacteria produce antibiotics, hydrolytic enzymes, and oxidative compounds to suppress competitors and gain access to limited nutrients (Amend et al. 2019; Wang and Kuzyakov 2024). This chemical interference occurs in parallel with direct resource competition, with both mechanisms

contributing to negative microbial interactions. Ascomycota exhibited negative interactions with Actinomycetota, particularly *Ilumatobacter* (No. 91 in Figure 6) and other Microtrichales (No. 78, 79, 199 in Figure 6; & No. 46, 49 in Figure 8), known for their antibiotic production. These bacteria produce non-ribosomal peptide synthetases that synthesize antimicrobial compounds (Ngamcharungchit et al. 2023), potentially suppressing fungal metabolism and colonization (Wohl and McArthur 2001). Negative connections between Bacteroidota and Ascomycota may be linked to bacterial beta-lactamase (Figure 10) found in Bacteroidales (OTU1900), Flavobacteriales (OTU113), and Cytophagales (OTU343, OTU5917, OTU93, OTU1217, OTU32) in NI–WB, which can neutralize beta-lactam-type antifungal agents (Mora-Ochomogo and Lohans 2021; Hudson and Egan 2022). In surface water networks (Figures 6 and 8), Gammaproteobacteria, such as Steroidobacterales, Chromatiales, Oceanospirillales, Cellvibrionales, B2M28 and Burkholderiales had many negative connections with Ascomycota, potentially linked to the production of reactive oxygen species via NADH oxidase, which can inhibit fungal growth (Diaz et al. 2013). Additionally, Comamonadaceae (Burkholderiales; OTU553, OTU409, OTU1267, OTU422), Burkholderiales (OTU202, OTU359, OTU1936, OTU61, OTU906, OTU187, OTU736), Cellvibrionales (OTU285), and Oceanospirillales (OTU384) are associated with beta-glucosidase and beta-lactamase pathways (Figure 10), suggesting that antagonism could combine chemical inhibition with enzymatic competition for carbohydrate-rich substrates also targeted by fungal saprotrophs (Figure 11). These antagonistic interactions can limit the dominance of individual taxa, maintaining microbial diversity and stabilizing community structure (Wang and Kuzyakov 2024).

Parasitism, particularly by early diverging fungi, further influences microbial interactions. Chytridiomycota, known parasites of phytoplankton, had negative connections with Cyanobacteriota (Figure 6; Leptolyngbyales No. 189 in Figure 6). Chytridiomycota and Blastocladiomycota are known to parasitize Cyanobacteriota, disrupting populations and enhancing nutrient turnover (Gerphagnon et al. 2019; Gleason et al. 2014; Sime-Ngando 2012). *Catenomyces* (Blastocladiomycota; No. 9 in Figure 5) and *Coelomomyces* (Blastocladiomycota; No. 8 in Figure 6) had negative connections with HOC36 (Gammaproteobacteria; No. 151 in Figure 6), and Chytridiomycota (No. 143 in Figure 6) also had negative connections with SAR11 (No. 32 in Figure 6). FUNGuild assignments (Figure S4; Dataset S1) confirm these groups' dual roles as litter saprotrophs and cyanobacterial parasites. In addition, their saprotrophic activity overlaps with SAR11 clade's ability to metabolize dissolved organic carbon (Alonso-Sáez and Gasol 2007; Denef et al. 2016; Sidhu et al. 2024), potentially intensifying competition for dissolved organic matter while simultaneously contributing to nutrient recycling (Amend et al. 2019; Peng et al. 2024).

4.5 | Potential Cross-Feeding and Nutrient Exchange

Alongside competitive and antagonistic interactions, the networks revealed positive associations indicative of functional cooperation and cross-feeding, where fungal enzymes initiate the breakdown of complex organic matter and bacterial enzymes further process the resulting compounds (Bärlocher and Boddy 2016; de Menezes et al. 2017; Amend et al. 2019; Wang and Kuzyakov 2024). In salt marsh sediments (Figure 6), Ascomycota and Blastocladiomycota had positive connections with Desulfobulbales (No. 168, 170, 177, 183 in Figure 6), suggesting metabolic exchange. The fungal guilds, including Sordariomycetes and Dothideomycetes litter and wood saprotrophs (Figure 11), likely release lignocellulose breakdown products that Desulfobulbales can metabolize during anaerobic respiration (Ferrari et al. 2021).

In both salt and brackish marsh surface waters (Figures 7 and 9), Ascomycota exhibited positive interactions with Gammaproteobacteria, particularly Oceanospirillales (No. 136 in Figure 7) and *Polynucleobacter* (Burkholderiales; No. 143 in Figure 7), *TRA3-20* (Burkholderiales; No. 114 in Figure 9), Comamonadaceae (Burkholderiales; No. 134 in Figure 7; No. 116 in Figure 9), and other Burkholderiales (No. 135, 139, 147 in Figure 7; & No. 96, 98, 99, 109, 110, 117, 120, 123, 134 in Figure 9). These interactions suggest that these bacteria may possess pathways for utilizing simple sugars and short-chain fatty acids, likely via beta-glucosidase (Figure 10), which may be supplied by fungal saprotroph activity (Figure 11). Such complementary metabolic roles can enhance organic matter degradation and nutrient regeneration in the water column (Bergfur and Friberg 2012). The prevalence of these positive connections in salt marsh sediment and surface waters further shows the complementary roles of fungi and bacteria in sustaining estuarine biogeochemistry.

In brackish marsh surface water (Figure 9), Ascomycota exhibited positive interactions with Rhizobiales (Alphaproteobacteria) that fix nitrogen. Groups in Rhizobiales, using nitrogenase (Figure 10), convert atmospheric nitrogen into ammonium (Kaneko et al. 2002; Bedmar et al. 2005), supporting fungal growth in nitrogen-limited environments. In return, Ascomycota likely release organic by-products that benefit Rhizobiales and other bacteria, promoting a mutualistic nutrient exchange (Rashid et al. 2016; Duan et al. 2018).

The co-occurrence network analysis showed positive connections between Chytridiomycota and Rhodobacterales (Alphaproteobacteria; No. 67 in Figure 6) in salt marsh sediment (Figure 6) and Flavobacteriales (No. 159 in Figure 9) in the brackish marsh surface water, suggesting enzymatic cooperation in polysaccharide degradation. Chytridiomycota, capable of breaking down complex polysaccharides such as starch and cellulose, release simpler sugars (Põlme et al. 2020) (Figure S4; Dataset S1) that Flavobacteriales and Rhodobacterales can metabolize further using beta-glucosidase (Figure 10), promoting organic matter turnover and facilitating nutrient cycling.

In salt marsh and brackish surface waters (Figures 6 and 9), Zoopagomycota had positive connections with Alphaproteobacteria and Actinomycetota, indicating potential co-metabolism of dissolved organic matter (DOM). Zoopagomycota, identified as saprotrophic fungi (Figure 11; Figure S4; Dataset S1), contribute to the degradation of organic substrates, releasing intermediates, such as lignocellulose derivatives and simple sugars (Větrovský et al. 2014; Chen

et al. 2025), that Alphaproteobacteria and Actinomycetota (No. 78, 60 in Figure 9) can further process as well as accelerating carbon turnover in the water column (de Menezes et al. 2017; Amend et al. 2019; Wang and Kuzyakov 2024). These cooperative interactions allow fungi and bacteria to partition resources, enhance nutrient availability, and maintain microbial diversity, ultimately driving key ecosystem processes such as carbon sequestration and nitrogen cycling (Kaneko et al. 2002; Bedmar et al. 2005; Griffiths and Philippot 2013; Toor et al. 2024; Wang and Kuzyakov 2024).

4.6 | Ecosystem Implications

Together, fungi and prokaryotes drive complementary biogeochemical processes in estuarine ecosystems, supporting nutrient cycling and organic matter decomposition (Amend et al. 2019; Peng et al. 2024; Wang and Kuzyakov 2024). These positive connections suggest metabolic complementarity through cross-feeding, co-metabolism, and nutrient exchange, all of which support organic matter breakdown, regulate nutrient cycling, and strengthen microbial resilience in dynamic environmental conditions (Li et al. 2015; van der Heijden et al. 2016; Amend et al. 2019; Wang and Kuzyakov 2024). Prokaryotes dominate sulfate reduction and DOC metabolism, while fungi focus on the breakdown of plant-derived organic material. Ultimately, the cooperative mechanisms observed between fungi and prokaryotes not only support microbial community dynamics but also have broader implications for the entire ecosystem. By enhancing organic matter decomposition, these interactions drive carbon turnover, which influences plant productivity and sediment stability (Buesing and Gessner 2006; Unger et al. 2016; Liang et al. 2023). Furthermore, microbial breakdown of organic material supports detrital food webs and impacts higher trophic levels, shaping the overall function of the estuarine ecosystem (Crump and Bowen 2024). The microbial processes in these marshes are foundational to ecosystem stability and productivity, with broader consequences for trophic energy flow and community interactions (Liang et al. 2023; Hu, Sun, et al. 2024).

However, competition between these groups is also evident, with both targeting shared resources such as DOC and nitrogen (Amend et al. 2019; Peng et al. 2024; Wang and Kuzyakov 2024). The absence of positive connections in brackish marsh sediment suggests that environmental factors such as salinity and resource competition may regulate cooperative dynamics. These cooperative and competitive interactions shape microbial community dynamics and are fundamental to the resilience and functionality of estuarine ecosystems (Wang et al. 2021; Wang and Kuzyakov 2024). While cooperation enhances system-level efficiency, competitive interactions can limit resource availability, constrain microbial diversity, and introduce trade-offs in metabolic pathways (Wang and Kuzyakov 2024). Such competition may reduce the efficiency of nutrient recycling under certain environmental conditions, potentially leading to localized bottlenecks in carbon turnover and nitrogen cycling (Li et al. 2020). These limitations can cascade upward, altering plant nutrient uptake, reducing primary productivity, and impacting the structure of detritus-based food webs (Calizza et al. 2015; Eldridge et al. 2017). Thus, the balance between cooperation and competition among microbial guilds plays a pivotal role in shaping both microbial community structure and broader estuarine ecosystem functionality.

4.7 | Environmental Variables Shape Microbial Interactions

Microbial connections in estuarine ecosystems vary between salt and brackish marshes, influenced by salinity and nutrient availability (Crain 2007; Mohamed and Martiny 2011; Rojas-Jimenez et al. 2019). Prokaryotic community composition differed between salt and brackish marshes, with Thousand Acre (brackish marsh) and Clambank (salt marsh) showing clear separation (Figure 4, PERMANOVA, $p = 0.001$, Table S2). The fungal community also exhibited significant differences between sites (Thompson et al. 2025), further underscoring the influence of environmental variables.

Salinity gradients play a critical role in structuring microbial communities and determining interaction dynamics. In the salt marsh, high salinity favors sulfate-reducing bacteria like Desulfobacteria, which may play a key role in anaerobic organic matter degradation (Demin et al. 2024; Magnuson et al. 2023). This environment fosters competition and cooperation with fungi, particularly Ascomycota. High salinity in the salt marsh promotes the dominance of Dikarya fungi (Ascomycota and Basidiomycota) (Figure 5), which may be adapted to salt stress and contribute to organic matter decomposition (Mohamed and Martiny 2011).

In contrast, lower salinity in the brackish marsh surface water allows for greater fungal diversity, enabling a wider range of competitive and cooperative interactions (Figure 5) (Thompson et al. 2025). The increased presence of early diverging fungi suggests a different ecological strategy, where these fungi may exploit diverse organic matter sources (Thompson et al. 2025). The absence of positive fungal-bacterial connections in the brackish marsh sediment further highlights the role of environmental conditions in shaping microbial community dynamics. Brackish marsh with lower salinity and higher nutrient levels supports a more diverse fungal and bacterial community (Figures 2 and 4) (Thompson et al. 2025). Early diverging fungi such as Zoopagomycota, Chytridiomycota, and Blastocladiomycota were dominant in the brackish marsh, suggesting their adaptation to fluctuating environmental conditions (Figure 5). While Ascomycota in the salt marsh had positive and negative connections with bacteria, fungal-bacterial connections in the brackish marsh sediment are nearly exclusively negative, indicating stronger competition for organic resources.

Nutrient availability in surface water is another key driver of fungal diversity, with nutrient-rich habitats supporting higher diversity. Such environments are known to foster greater diversity in both planktonic fungal communities (Jeffries et al. 2016) and benthic fungal communities in marsh sediments (Kearns et al. 2019). In the brackish marsh surface water, where nutrient concentrations were high (Figure 2), positive connections outweighed negative connections, in contrast to all other networks. The increased nutrient availability may lessen competition for limited resources in surface waters, allowing fungi and bacteria to specialize in different functions rather than

directly competing (Lin et al. 2021; Hu, Zhou, et al. 2024; Wang and Kuzyakov 2024). In contrast, the negative interactions in the brackish marsh sediment may be a result of close physical proximity (Ghoul and Mitri 2016; Martinez-Rabert et al. 2022). Ultimately, the balance between cooperative and antagonistic interactions among microbial communities is central to the ecological functioning of salt marshes, helping stabilize sediments and sustain biodiversity.

5 | Conclusions

The interactions between fungi and bacteria in estuarine ecosystems are shaped by a complex balance of competition and cooperation, influenced by environmental factors such as salinity and nutrient flux (Mohamed and Martiny 2011; Tee et al. 2021; Xu et al. 2025). These factors influence the extent to which microbial communities engage in resource competition, antagonistic interactions, or cooperative processes including cross-feeding, co-metabolism, and enzymatic complementarity (Amend et al. 2019; Dong et al. 2022; Peng et al. 2024; Wang and Kuzyakov 2024). Cooperative interactions can enhance organic matter decomposition, nutrient retention, and sediment stability, while competitive dynamics may limit nutrient recycling efficiency and alter microbial diversity (Pawlowska 2024; Wang and Kuzyakov 2024).

Understanding these dynamics has implications beyond the microbial scale. Because fungal–bacterial interactions regulate carbon turnover, nitrogen cycling, and sediment cohesion (Fabian et al. 2017; Romoth et al. 2023; Pawlowska 2024; Wang and Kuzyakov 2024), shifts in the balance between cooperation and competition could cascade to affect primary production, detrital food web structure, and overall estuarine resilience to disturbance (Hestrin et al. 2019; Wang and Kuzyakov 2024). Projected climate-driven changes in sea level, salinity regimes, and nutrient loading are likely to alter these interaction networks, with consequences for coastal carbon storage, nutrient flux to adjacent waters, and habitat quality for higher trophic levels (Philippot et al. 2021; Walker et al. 2022; Wang and Kuzyakov 2024). Recognizing how these relationships respond to environmental change will be critical for refining biogeochemical models, guiding restoration strategies that maintain functional microbial diversity, and predicting the long-term stability of blue carbon ecosystems under shifting climate and land-use conditions.

Author Contributions

Madeleine A. Thompson: conceptualization, data curation, formal analysis, investigation, methodology, software, validation, visualization, writing – original draft, writing – review and editing. **Xuefeng Peng:** conceptualization, data curation, formal analysis, funding acquisition, investigation, methodology, project administration, resources, supervision, validation, writing – review and editing.

Acknowledgments

We thank Birch Lazo-Murphy for assisting with sample collection. This is contribution number 1927 of the Belle W. Baruch Institute for Marine and Coastal Sciences of the University of South Carolina.

Conflicts of Interest

The authors declare no conflicts of interest.

Data Availability Statement

Raw reads generated in this study are available at the National Center for Biotechnology Information (NCBI) under BioProject PRJNA1158776. All code is available at GitHub: https://github.com/mthompson19/Interactions-and-Community-Structure-of-Fungi-and-Prokaryotes-in-Salt-and-Brackish-Marsh-Ecosystems.

References

Agha, R., M. Saebelfeld, C. Manthey, T. Rohrlack, and J. Wolinska. 2016. "Chytrid Parasitism Facilitates Trophic Transfer Between Bloom-Forming Cyanobacteria and Zooplankton (Daphnia)." *Scientific Reports* 6: 35039.

Allen, D., W. Allen, R. Feller, et al. 2014. *Site Profile of the North Inlet–Winyah Bay National Estuarine Research Reserve*. Vol. 432. North Inlet–Winyah Bay National Estuarine Research Reserve.

Alonso-Sáez, L., and J. M. Gasol. 2007. "Seasonal Variations in the Contributions of Different Bacterial Groups to the Uptake of Low-Molecular-Weight Compounds in Northwestern Mediterranean Coastal Waters." *Applied and Environmental Microbiology* 73: 3528–3535.

Ameen, M., A. Mahmood, A. Sahkoor, M. A. Zia, and M. S. Ullah. 2024. "The Role of Endophytes to Combat Abiotic Stress in Plants." *Plant Stress* 12: 100435.

Amend, A., G. Burgaud, M. Cunliffe, et al. 2019. "Fungi in the Marine Environment: Open Questions and Unsolved Problems." *MBio* 10: e01189-18.

Banerjee, S., K. Schlaeppi, and M. G. A. Van Der Heijden. 2018. "Keystone Taxa as Drivers of Microbiome Structure and Functioning." *Nature Reviews. Microbiology* 16: 567–576.

Barbier, E. B., S. D. Hacker, C. Kennedy, E. W. Koch, A. C. Stier, and B. R. Silliman. 2011. "The Value of Estuarine and Coastal Ecosystem Services." *Ecological Monographs* 81: 169–193.

Bärlocher, F., and L. Boddy. 2016. "Aquatic Fungal Ecology–How Does It Differ From Terrestrial?" *Fungal Ecology* 19: 5–13.

Bedmar, E. J., E. F. Robles, and M. J. Delgado. 2005. "The Complete Denitrification Pathway of the Symbiotic, Nitrogen-Fixing Bacterium *Bradyrhizobium japonicum*." *Biochemical Society Transactions* 33: 141–144.

Behera, A. D., and S. Das. 2023. "Ecological Insights and Potential Application of Marine Filamentous Fungi in Environmental Restoration." *Reviews in Environmental Science and Bio/Technology* 22: 281–318.

Bell, E., T. Lamminmäki, J. Alneberg, et al. 2022. "Active Anaerobic Methane Oxidation and Sulfur Disproportionation in the Deep Terrestrial Subsurface." *ISME Journal* 16: 1583–1593.

Bergfur, J., and N. Friberg. 2012. "Trade-Offs Between Fungal and Bacterial Respiration Along Gradients in Temperature, Nutrients and Substrata: Experiments With Stream Derived Microbial Communities." *Fungal Ecology* 5: 46–52.

Blum, L. K., and A. L. Mills. 2012. "Estuarine Microbial Ecology." In *Estuarine Ecology*, 235–261. Wiley-Blackwell.

Boer, W., L. B. Folman, R. C. Summerbell, et al. 2005. "Living in a Fungal World: Impact of Fungi on Soil Bacterial Niche Development." *FEMS Microbiology Reviews* 29: 795–811.

Bolger, A. M., M. Lohse, and B. Usadel. 2014. "Trimmomatic: A Flexible Trimmer for Illumina Sequence Data." *Bioinformatics* 30: 2114–2120.

Braatz, S., S. Fortuna, J. Broadhead, et al. 2007. "Proceedings of the Regional Technical Workshop, Khao Lak, Thailand, 28–31 August 2006." In *Coastal Protection in the Aftermath of the Indian Ocean Tsunami: What Role for Forests and Trees?* edited by S. Braatz, S. F. J. Broadhead, and R. Leslieeditors, 220. FAO Regional Office for Asia and the Pacific.

Buesing, N., and M. O. Gessner. 2006. "Benthic Bacterial and Fungal Productivity and Carbon Turnover in a Freshwater Marsh." *Applied and Environmental Microbiology* 72: 596–605.

Bushnell, B., J. Rood, and E. Singer. 2017. "BBMerge–Accurate Paired Shotgun Read Merging via Overlap." *PLoS One* 12: e0185056.

Calabon, M. S., E. G. Jones, I. Promputtha, et al. 2021. "Fungal Biodiversity in Salt Marsh Ecosystems." *Journal of Fungi* 7: 648.

Calizza, E., M. L. Costantini, and L. Rossi. 2015. "Effect of Multiple Disturbances on Food Web Vulnerability to Biodiversity Loss in Detritus-Based Systems." *Ecosphere* 6: 1–20.

Cameron, E. S., P. J. Schmidt, B. J.-M. Tremblay, M. B. Emelko, and K. M. Müller. 2021. "Enhancing Diversity Analysis by Repeatedly Rarefying Next Generation Sequencing Data Describing Microbial Communities." *Scientific Reports* 11: 22302.

Caporaso, J. G., J. Kuczynski, J. Stombaugh, et al. 2010. "QIIME Allows Analysis of High-Throughput Community Sequencing Data." *Nature Methods* 7: 335–336.

Carlson, C. A., and J. L. Ingraham. 1983. "Comparison of Denitrification by *Pseudomonas stutzeri*, Pseudomonas Aeruginosa, and *Paracoccus denitrificans*." *Applied and Environmental Microbiology* 45: 1247–1253.

Carrasco-Barea, L., L. Llorens, A. M. Romaní, M. Gispert, and D. Verdaguer. 2022. "Litter Decomposition of Three Halophytes in a Mediterranean Salt Marsh: Relevance of Litter Quality, Microbial Activity and Microhabitat." *Science of the Total Environment* 838: 155743.

Carstensen, J., R. Klais, and J. E. Cloern. 2015. "Phytoplankton Blooms in Estuarine and Coastal Waters: Seasonal Patterns and Key Species." *Estuarine, Coastal and Shelf Science* 162: 98–109.

Chavda, N. D., H. N. Deota, and V. K. B. Kota. 2014. "Poisson to GOE Transition in the Distribution of the Ratio of Consecutive Level Spacings." *Physics Letters A* 378: 3012–3017.

Chen, M., Q. Li, C. Liu, E. Meng, and B. Zhang. 2025. "Microbial Degradation of Lignocellulose for Sustainable Biomass Utilization and Future Research Perspectives." *Sustainability* 17: 4223. https://doi.org/10.3390/su17094223.

Comeau, A. M., W. F. Vincent, L. Bernier, and C. Lovejoy. 2016. "Novel Chytrid Lineages Dominate Fungal Sequences in Diverse Marine and Freshwater Habitats." *Scientific Reports* 6: 30120.

Crain, C. M. 2007. "Shifting Nutrient Limitation and Eutrophication Effects in Marsh Vegetation Across Estuarine Salinity Gradients." *Estuaries and Coasts* 30: 26–34.

Crump, B. C., and J. L. Bowen. 2024. "The Microbial Ecology of Estuarine Ecosystems." *Annual Review of Marine Science* 16: 335–360.

Czapla, K. M., I. C. Anderson, and C. A. Currin. 2020. "Net Ecosystem Carbon Balance in a North Carolina, USA, Salt Marsh." *Journal of Geophysical Research–Biogeosciences* 125: e2019JG005509.

de Menezes, A. B., A. E. Richardson, and P. H. Thrall. 2017. "Linking Fungal–Bacterial Co-Occurrences to Soil Ecosystem Function." *Current Opinion in Microbiology* 37: 135–141.

Deegan, L., J. Bowen, D. Drake, et al. 2007. "Susceptibility of Salt Marshes to Nutrient Enrichment and Predator Removal." *Ecological Applications* 17: S42–S63. https://doi.org/10.1890/06-0452.1.

Demin, K. A., E. V. Prazdnova, T. M. Minkina, and A. V. Gorovtsov. 2024. "Sulfate-Reducing Bacteria Unearthed: Ecological Functions of the Diverse Prokaryotic Group in Terrestrial Environments." *Applied and Environmental Microbiology* 90: e01390-23.

Denef, V. J., R. S. Mueller, E. Chiang, J. R. Liebig, and H. A. Vanderploeg. 2016. "Chloroflexi CL500-11 Populations That Predominate Deep-Lake Hypolimnion Bacterioplankton Rely on Nitrogen-Rich Dissolved Organic Matter Metabolism and C1 Compound Oxidation." *Applied and Environmental Microbiology* 82: 1423–1432.

Deng, Y., Y.-H. Jiang, Y. Yang, Z. He, F. Luo, and J. Zhou. 2012. "Molecular Ecological Network Analyses." *BMC Bioinformatics* 13: 113.

Diaz, J. M., C. M. Hansel, B. M. Voelker, C. M. Mendes, P. F. Andeer, and T. Zhang. 2013. "Widespread Production of Extracellular Superoxide by Heterotrophic Bacteria." *Science* 340: 1223–1226.

Dini-Andreote, F., M. de Cássia Pereira e Silva, X. Triadó-Margarit, E. O. Casamayor, J. D. van Elsas, and J. F. Salles. 2014. "Dynamics of Bacterial Community Succession in a Salt Marsh Chronosequence: Evidences for Temporal Niche Partitioning." *ISME Journal* 8: 1989–2001.

Dong, Y., J. Zhang, R. Chen, L. Zhong, X. Lin, and Y. Feng. 2022. "Microbial Community Composition and Activity in Saline Soils of Coastal Agro–Ecosystems." *Microorganisms* 10: 835.

Douglas, G., V. Maffei, J. Zaneveld, et al. 2020. "PICRUSt2: An Improved and Extensible Approach for Metagenome Inference." *Nat Biotechnol* 38, no. 6: 685–688. https://doi.org/10.1038/s41587-020-0548-6.

Duan, Y., N. Xie, Z. Song, et al. 2018. "A High-Resolution Time Series Reveals Distinct Seasonal Patterns of Planktonic Fungi at a Temperate Coastal Ocean Site (Beaufort, North Carolina, USA)." *Applied and Environmental Microbiology* 84: e00967-18.

Edgar, R. C. 2010. "Search and Clustering Orders of Magnitude Faster Than BLAST." *Bioinformatics* 26: 2460–2461.

Eldridge, D. J., M. Delgado-Baquerizo, S. K. Travers, et al. 2017. "Competition Drives the Response of Soil Microbial Diversity to Increased Grazing by Vertebrate Herbivores." *Ecology* 98: 1922–1931.

Fabian, J., S. Zlatanovic, M. Mutz, and K. Premke. 2017. "Fungal–Bacterial Dynamics and Their Contribution to Terrigenous Carbon Turnover in Relation to Organic Matter Quality." *ISME Journal* 11: 415–425.

Ferrari, R., V. Gautier, and P. Silar. 2021. "Chapter Three-Lignin Degradation by Ascomycetes." In *Advances in Botanical Research*, edited by M. Morel-Rouhier and R. Sormani, vol. 99, 77–113. Academic Press.

Flood, B. E., D. S. Jones, and J. V. Bailey. 2015. "Sedimenticola Thiotaurini sp. nov., a Sulfur-Oxidizing Bacterium Isolated From Salt Marsh Sediments, and Emended Descriptions of the Genus Sedimenticola and *Sedimenticola selenatireducens*." *International Journal of Systematic and Evolutionary Microbiology* 65: 2522–2530.

Friedman, J., and E. J. Alm. 2012. "Inferring Correlation Networks From Genomic Survey Data." *PLoS Computational Biology* 8: e1002687.

Ge, H., C. Li, C. Huang, L. Zhao, B. Cong, and S. Liu. 2025. "Bacterial Community Composition and Metabolic Characteristics of Three Representative Marine Areas in Northern China." *Marine Environmental Research* 204: 106892.

Gerphagnon, M., R. Agha, D. Martin-Creuzburg, et al. 2019. "Comparison of Sterol and Fatty Acid Profiles of Chytrids and Their Hosts Reveals Trophic Upgrading of Nutritionally Inadequate Phytoplankton by Fungal Parasites." *Environmental Microbiology* 21: 949–958.

Ghoul, M., and S. Mitri. 2016. "The Ecology and Evolution of Microbial Competition." *Trends in Microbiology* 24: 833–845.

Gleason, F. H., A. Chambouvet, B. K. Sullivan, O. Lilje, and J. J. L. Rowley. 2014. "Multiple Zoosporic Parasites Pose a Significant Threat to Amphibian Populations." *Fungal Ecology* 11: 181–192.

Griffiths, B. S., and L. Philippot. 2013. "Insights Into the Resistance and Resilience of the Soil Microbial Community." *FEMS Microbiology Reviews* 37: 112–129.

Guimerà, R., and L. A. N. Amaral. 2005. "Cartography of Complex Networks: Modules and Universal Roles." *Journal of Statistical Mechanics: Theory and Experiment* 2005: P02001.

Guo, X., W. Peng, X. Xu, K. Xie, and X. Yang. 2023. "The Potential of Endophytes in Improving Salt–Alkali Tolerance and Salinity Resistance in Plants." *IJMS* 24: 16917.

Hestrin, R., E. C. Hammer, C. W. Mueller, and J. Lehmann. 2019. "Synergies Between Mycorrhizal Fungi and Soil Microbial Communities Increase Plant Nitrogen Acquisition." *Communications Biology* 2: 233.

Hu, D., X. Zhou, G. Ma, et al. 2024. "Increased Soil Bacteria-Fungus Interactions Promote Soil Nutrient Availability, Plant Growth, and Coexistence." *Science of the Total Environment* 955: 176919.

Hu, M., D. Sun, J. Sardans, et al. 2024. "Bacterial and Fungal Communities Exhibit Contrasting Patterns in Response to Marsh Erosion: A Fine-Scale Observation." *Catena* 244: 108231.

Hudson, J., and S. Egan. 2022. "Opportunistic Diseases in Marine Eukaryotes: Could Bacteroidota Be the Next Threat to Ocean Life?" *Environmental Microbiology* 24: 4505–4518.

Jeffries, T. C., N. J. Curlevski, M. V. Brown, et al. 2016. "Partitioning of Fungal Assemblages Across Different Marine Habitats." *Environmental Microbiology Reports* 8: 235–238.

Jin, R., T. Liu, G. Liu, J. Zhou, J. Huang, and A. Wang. 2015. "Simultaneous Heterotrophic Nitrification and Aerobic Denitrification by the Marine Origin Bacterium Pseudomonas sp. ADN-42." *Applied Biochemistry and Biotechnology* 175: 2000–2011.

Jones, E. G. 2011. "Fifty Years of Marine Mycology." *Fungal Diversity* 50: 73–112.

Kaneko, T., Y. Nakamura, S. Sato, et al. 2002. "Complete Genomic Sequence of Nitrogen-Fixing Symbiotic Bacterium *Bradyrhizobium japonicum* USDA110." *DNA Research* 9: 189–197.

Kearns, P. J., A. N. Bulseco-McKim, H. Hoyt, J. H. Angell, and J. L. Bowen. 2019. "Nutrient Enrichment Alters Salt Marsh Fungal Communities and Promotes Putative Fungal Denitrifiers." *Microbial Ecology* 77: 358–369.

Ketudat Cairns, J. R., and A. Esen. 2010. "β-Glucosidases." *Cellular and Molecular Life Sciences* 67: 3389–3405.

Kong, L.-F., Y.-B. He, Z.-X. Xie, et al. 2021. "Illuminating Key Microbial Players and Metabolic Processes Involved in the Remineralization of Particulate Organic Carbon in the Ocean's Twilight Zone by Metaproteomics." *Applied and Environmental Microbiology* 87: e00986-21.

Kurtz, Z. D., C. L. Müller, E. R. Miraldi, D. R. Littman, M. J. Blaser, and R. A. Bonneau. 2015. "Sparse and Compositionally Robust Inference of Microbial Ecological Networks." *PLoS Computational Biology* 11: e1004226.

Langfelder, P., and S. Horvath. 2008. "WGCNA: An R Package for Weighted Correlation Network Analysis." *BMC Bioinformatics* 9: 559.

Leadbeater, D. R., N. C. Oates, J. P. Bennett, et al. 2021. "Mechanistic Strategies of Microbial Communities Regulating Lignocellulose Deconstruction in a UK Salt Marsh." *Microbiome* 9: 48.

Li, H., C. Wang, Q. Yu, and E. Smith. 2022. "Spatiotemporal Assessment of Potential Drivers of Salt Marsh Dieback in the North Inlet-Winyah Bay Estuary, South Carolina (1990–2019)." *Journal of Environmental Management* 313: 114907.

Li, J., L. Cui, M. Delgado-Baquerizo, et al. 2022. "Fungi Drive Soil Multifunctionality in the Coastal Salt Marsh Ecosystem." *Science of the Total Environment* 818: 151673.

Li, X., L. Hou, M. Liu, X. Lin, Y. Li, and S. Li. 2015. "Primary Effects of Extracellular Enzyme Activity and Microbial Community on Carbon and Nitrogen Mineralization in Estuarine and Tidal Wetlands." *Applied Microbiology and Biotechnology* 99: 2895–2909.

Li, Z., B. Liu, S. H.-J. Li, et al. 2020. "Modeling Microbial Metabolic Trade-Offs in a Chemostat." *PLoS Computational Biology* 16: e1008156.

Liang, S., H. Li, H. Wu, B. Yan, and A. Song. 2023. "Microorganisms in Coastal Wetland Sediments: A Review on Microbial Community Structure, Functional Gene, and Environmental Potential." *Frontiers in Microbiology* 14: 1163896.

Lin, Q., L. Li, J. M. Adams, et al. 2021. "Nutrient Resource Availability Mediates Niche Differentiation and Temporal Co-Occurrence of Soil Bacterial Communities." *Applied Soil Ecology* 163: 103965.

Magnuson, E., I. Altshuler, N. J. Freyria, R. J. Leveille, and L. G. Whyte. 2023. "Sulfur-Cycling Chemolithoautotrophic Microbial Community Dominates a Cold, Anoxic, Hypersaline Arctic Spring." *Microbiome* 11: 203.

Martinez-Rabert, E., C. Van Amstel, C. Smith, et al. 2022. "Environmental and Ecological Controls of the Spatial Distribution of Microbial Populations in Aggregates." *PLoS Computational Biology* 18: e1010807.

Mcleod, E., G. L. Chmura, S. Bouillon, et al. 2011. "A Blueprint for Blue Carbon: Toward an Improved Understanding of the Role of Vegetated Coastal Habitats in Sequestering CO_2." *Frontiers in Ecology and the Environment* 9: 552–560.

McMurdie, P. J., and S. Holmes. 2013. "Phyloseq: An R Package for Reproducible Interactive Analysis and Graphics of Microbiome Census Data." *PLoS One* 8: e61217.

Mohamed, D. J., and J. B. H. Martiny. 2011. "Patterns of Fungal Diversity and Composition Along a Salinity Gradient." *ISME Journal* 5: 379–388.

Mora-Ochomogo, M., and C. T. Lohans. 2021. "β-Lactam Antibiotic Targets and Resistance Mechanisms: From Covalent Inhibitors to Substrates." *RSC Medicinal Chemistry* 12: 1623–1639.

Murrell, M. C., and E. M. Lores. 2004. "Phytoplankton and Zooplankton Seasonal Dynamics in a Subtropical Estuary: Importance of Cyanobacteria." *Journal of Plankton Research* 26: 371–382.

Myers, J. M., A. E. Bonds, R. A. Clemons, et al. 2020. "Survey of Early-Diverging Lineages of Fungi Reveals Abundant and Diverse Mycoviruses." *MBio* 11: e02027-20. https://doi.org/10.1128/mbio.02027-20.

Ngamcharungchit, C., N. Chaimusik, W. Panbangred, J. Euanorasetr, and B. Intra. 2023. "Bioactive Metabolites From Terrestrial and Marine Actinomycetes." *Molecules* 28: 5915. https://doi.org/10.3390/molecules28155915.

Nguyen, N. H., Z. Song, S. T. Bates, et al. 2016. "FUNGuild: An Open Annotation Tool for Parsing Fungal Community Datasets by Ecological Guild." *Fungal Ecology* 20: 241–248.

Parada, A. E., D. M. Needham, and J. A. Fuhrman. 2015. "Every Base Matters: Assessing Small Subunit rRNA Primers for Marine Microbiomes With Mock Communities, Time Series and Global Field Samples." *Environmental Microbiology* 18, no. 5: 1403–1414. https://doi.org/10.1111/1462-2920.13023.

Patchineelam, S. M., B. Kjerfve, and L. R. Gardner. 1999. "A Preliminary Sediment Budget for the Winyah Bay Estuary, South Carolina, USA." *Marine Geology* 162: 133–144.

Pawlowska, T. E. 2024. "Symbioses Between Fungi and Bacteria: From Mechanisms to Impacts on Biodiversity." *Current Opinion in Microbiology* 80: 102496.

Peng, X., A. S. Amend, F. Baltar, et al. 2024. "Planktonic Marine Fungi: A Review." *Journal of Geophysical Research–Biogeosciences* 129: e2023JG007887.

Peng, X., and D. L. Valentine. 2021. "Diversity and N_2O Production Potential of Fungi in an Oceanic Oxygen Minimum Zone." *Journal of Fungi* 7, no. 3: 218. https://doi.org/10.3390/jof7030218.

Pham, T. T., K. V. Dinh, and V. D. Nguyen. 2021. "Biodiversity and Enzyme Activity of Marine Fungi With 28 New Records From the Tropical Coastal Ecosystems in Vietnam." *Mycobiology* 49: 559–581.

Philippot, L., B. S. Griffiths, and S. Langenheder. 2021. "Microbial Community Resilience Across Ecosystems and Multiple Disturbances." *Microbiology and Molecular Biology Reviews* 85. https://doi.org/10.1128/mmbr.00026-20.

Picard, K. T. 2017. "Coastal Marine Habitats Harbor Novel Early-Diverging Fungal Diversity." *Fungal Ecology* 25: 1–13.

Põlme, S., K. Abarenkov, R. Henrik Nilsson, et al. 2020. "FungalTraits: A User-Friendly Traits Database of Fungi and Fungus-Like Stramenopiles." *Fungal Diversity* 105: 1–16.

QIAGEN. 2023. "DNeasy PowerSoil Pro Kit Handbook." https://www.qiagen.com/us/resources/resourcedetail?id=9bb59b74-e493-4aeb-b6c1-f660852e8d97&lang=en.

Qian, L., X. Yu, H. Gu, et al. 2023. "Vertically Stratified Methane, Nitrogen and Sulphur Cycling and Coupling Mechanisms in Mangrove Sediment Microbiomes." *Microbiome* 11: 71.

Quast, C., E. Pruesse, P. Yilmaz, et al. 2012. "The SILVA Ribosomal RNA Gene Database Project: Improved Data Processing and Web-Based Tools." *Nucleic Acids Research* 41: D590–D596.

Rasconi, S., M. Jobard, L. Jouve, and T. Sime-Ngando. 2009. "Use of Calcofluor White for Detection, Identification, and Quantification of Phytoplanktonic Fungal Parasites." *Applied and Environmental Microbiology* 75: 2545–2553.

Rashid, M. I., L. H. Mujawar, T. Shahzad, T. Almeelbi, I. M. I. Ismail, and M. Oves. 2016. "Bacteria and Fungi Can Contribute to Nutrients Bioavailability and Aggregate Formation in Degraded Soils." *Microbiological Research* 183: 26–41.

Rojas-Jimenez, K., A. Rieck, C. Wurzbacher, K. Jürgens, M. Labrenz, and H. P. Grossart. 2019. "A Salinity Threshold Separating Fungal Communities in the Baltic Sea." *Frontiers in Microbiology* 10: 680.

Romoth, K., A. Darr, S. Papenmeier, M. L. Zettler, and M. Gogina. 2023. "Substrate Heterogeneity as a Trigger for Species Diversity in Marine Benthic Assemblages." *Biology* 12: 825.

Röttjers, L., and K. Faust. 2018. "From Hairballs to Hypotheses–Biological Insights From Microbial Networks." *FEMS Microbiology Reviews* 42: 761–780.

Sen, K., B. Sen, and G. Wang. 2022. "Diversity, Abundance, and Ecological Roles of Planktonic Fungi in Marine Environments." *Journal of Fungi* 8: 491. https://doi.org/10.3390/jof8050491.

Shannon, P., A. Markiel, O. Ozier, et al. 2003. "Cytoscape: A Software Environment for Integrated Models of Biomolecular Interaction Networks." *Genome Research* 13: 2498–2504.

Shepard, C. C., C. M. Crain, and M. W. Beck. 2011. "The Protective Role of Coastal Marshes: A Systematic Review and Meta-Analysis." *PLoS One* 6: e27374.

Sidhu, C., D. Bartosik, V. Kale, et al. 2024. "Resource Partitioning in Organosulfonate Utilization by Free-Living Heterotrophic Bacteria During a North Sea Microalgal Bloom." *BioRxiv*: 2024.12.10.627767.

Simas, T., J. P. Nunes, and J. G. Ferreira. 2001. "Effects of Global Climate Change on Coastal Salt Marshes." *Ecological Modelling* 139: 1–15.

Sime-Ngando, T. 2012. "Phytoplankton Chytridiomycosis: Fungal Parasites of Phytoplankton and Their Imprints on the Food Web Dynamics." *Frontiers in Microbiology* 3: 361.

Tebbe, D. A., S. Geihser, B. Wemheuer, R. Daniel, H. Schäfer, and B. Engelen. 2022. "Seasonal and Zonal Succession of Bacterial Communities in North Sea Salt Marsh Sediments." *Microorganisms* 10: 859. https://doi.org/10.3390/microorganisms10050859.

Tedersoo, L., S. Anslan, M. Bahram, et al. 2015. "Shotgun Metagenomes and Multiple Primer Pair-Barcode Combinations of Amplicons Reveal Biases in Metabarcoding Analyses of Fungi." *MycoKeys* 10: 1–43. https://doi.org/10.3897/mycokeys.10.4852.

Tee, H. S., D. Waite, G. Lear, and K. M. Handley. 2021. "Microbial River-to-Sea Continuum: Gradients in Benthic and Planktonic Diversity, Osmoregulation and Nutrient Cycling." *Microbiome* 9: 190.

Thompson, M. A., B. M. Lazo-Murphy, B. W. Pfirrmann, W. H. J. Strosnider, J. L. Pinckney, and X. Peng. 2025. "Beyond Dikarya: 28S Metabarcoding Uncovers Cryptic Fungal Lineages Across a Tidal Estuary." *Environmental Microbiomes* 20, no. 1: 129. https://doi.org/10.1186/s40793-025-00786-3.

Toor, M. D., M. Ur Rehman, J. Abid, et al. 2024. "Microbial Ecosystems as Guardians of Food Security and Water Resources in the Era of Climate Change." *Water, Air, & Soil Pollution* 235: 741.

Unger, V., T. Elsey-Quirk, C. Sommerfield, and D. Velinsky. 2016. "Stability of Organic Carbon Accumulating in *Spartina alterniflora*-Dominated Salt Marshes of the Mid-Atlantic U.S." *Estuarine, Coastal and Shelf Science* 182: 179–189.

van der Heijden, M. G. A., S. de Bruin, L. Luckerhoff, R. S. P. van Logtestijn, and K. Schlaeppi. 2016. "A Widespread Plant-Fungal-Bacterial Symbiosis Promotes Plant Biodiversity, Plant Nutrition and Seedling Recruitment." *ISME Journal* 10: 389–399.

Větrovský, T., K. T. Steffen, P. Baldrian, et al. 2014. "Potential of Cometabolic Transformation of Polysaccharides and Lignin in Lignocellulose by Soil Actinobacteria." *PLoS One* 9: e89108.

Walker, J. R., A. C. Woods, M. K. Pierce, et al. 2022. "Functionally Diverse Microbial Communities Show Resilience in Response to a Record-Breaking Rain Event." *ISME Communications* 2: 81. https://doi.org/10.1038/s43705-022-00162-z.

Wang, C., and Y. Kuzyakov. 2024. "Mechanisms and Implications of Bacterial–Fungal Competition for Soil Resources." *ISME Journal* 18: wrae073.

Wang, H., F. Chen, C. Zhang, M. Wang, and J. Kan. 2021. "Estuarine Gradients Dictate Spatiotemporal Variations of Microbiome Networks in the Chesapeake Bay." *Environmental Microbiomes* 16: 22.

Wang, M., W. Zhang, W. Xu, Y. Shen, and L. du. 2016. "Optimization of Genome Shuffling for High-Yield Production of the Antitumor Deacetylmycoepoxydiene in an Endophytic Fungus of Mangrove Plants." *Applied Microbiology and Biotechnology* 100: 7491–7498.

Wang, Q., and J. R. Cole. 2024. "Updated RDP Taxonomy and RDP Classifier for More Accurate Taxonomic Classification." *Microbiology Resource Announcements* 13: e01063-23.

Wang, Q., G. M. Garrity, J. M. Tiedje, and J. R. Cole. 2007. "Naïve Bayesian Classifier for Rapid Assignment of rRNA Sequences Into the New Bacterial Taxonomy." *Applied and Environmental Microbiology* 73: 5261–5267.

Wang, Y., Y. Chang, J. Ortañez, et al. 2023. "Divergent Evolution of Early Terrestrial Fungi Reveals the Evolution of Mucormycosis Pathogenicity Factors." *Genome Biology and Evolution*: 15, no. 4: evad046. https://doi.org/10.1093/gbe/evad046.

Watanabe, T., H. Kojima, and M. Fukui. 2016. "Identity of Major Sulfur-Cycle Prokaryotes in Freshwater Lake Ecosystems Revealed by a Comprehensive Phylogenetic Study of the Dissimilatory Adenylylsulfate Reductase." *Scientific Reports* 6: 36262.

Wohl, D. L., and J. V. McArthur. 2001. "Aquatic Actinomycete-Fungal Interactions and Their Effects on Organic Matter Decomposition: A Microcosm Study." *Microbial Ecology* 42: 446–457.

Xiao, N., A. Zhou, M. L. Kempher, et al. 2022. "Disentangling Direct From Indirect Relationships in Association Networks." *Proceedings of the National Academy of Sciences of the United States of America* 119: e2109995119.

Xu, J., L. Chen, T. Zhou, C. Zhang, J. Zhang, and B. Zhao. 2025. "Salinity-Driven Differentiation of Bacterial and Fungal Communities in Coastal Wetlands: Contrasting Assembly Processes and Spatial Dynamics." *Environmental Research* 279: 121895.

Zhang, G., J. Bai, Y. Zhai, et al. 2024. "Microbial Diversity and Functions in Saline Soils: A Review From a Biogeochemical Perspective." *Journal of Advanced Research* 59: 129–140.

Zhou, J., Y. Deng, F. Luo, et al. 2010. "Functional Molecular Ecological Networks." *MBio* 1: e00169-10.

Zhou, J., Y. Deng, F. Luo, et al. 2011. "Phylogenetic Molecular Ecological Network of Soil Microbial Communities in Response to Elevated CO_2." *mBio* 2: e00122-11.

Supporting Information

Additional supporting information can be found online in the Supporting Information section. **Dataset: S1.** Fungal OTUs present in each network analysis (separated by different tabs) with the full taxonomy assigned by RDP and functions assigned by FUNGuild. **Dataset: S2.** PICRUSt2 assignments, EC numbers, and estimated function abundance for all prokaryotic OTUs from Clambank (CB) sediment (S) samples. **Dataset: S3.** PICRUSt2 assignments, EC numbers, and estimated function abundance for all prokaryotic OTUs from Clambank (CB) surface water (WF) samples. **Dataset: S4.** PICRUSt2 assignments, EC numbers, and estimated function abundance for all prokaryotic OTUs from Thousand Acre (TA) sediment (S) samples. **Dataset: S5.** PICRUSt2 assignments, EC numbers, and estimated function abundance for all prokaryotic OTUs from Thousand Acre (TA) surface water (WF) samples. **Dataset: S6.** Mean and maximum relative abundance for all "Other" phyla (from Figure 3) per sample type (sediment and surface water) and station (Clambank [CB], Oyster Landing [OL], Debidue Creek [DB], and Thousand Acre [TA]). **Dataset: S7.** The OTUs present in the Clambank sediment network with their respective network number and full taxonomy. **Dataset: S8.** The OTUs present in the Clambank surface water network with their respective network number and full taxonomy. **Dataset: S9.** The OTUs present in the Thousand Acre sediment network with their respective network number and full taxonomy. **Dataset: S10.** The OTUs present in the Thousand Acre surface water network with their respective network number and full taxonomy. **Figure S1:** Relative abundance of Alphaproteobacteria orders across all sampling dates (June 2020, August 2020, February 2021, and November 2021) in: (A) sediment, Clambank; (B) surface water, Clambank; (C) sediment, Debidue Creek; (D) surface water, Debidue Creek; (E) sediment, Oyster Landing; (F) surface water, Oyster Landing; (G) sediment, Thousand Acre; and (H) surface water, Thousand Acre. Data are shown for biological replicates R1, R2, and R3. Orders representing $<0.5\%$ of relative abundance across all samples were grouped as "Other_Order." **Figure S2:** Relative abundance of Bacteroidota orders across all sampling dates (June 2020, August 2020, February 2021, and November 2021) in: (A) sediment, Clambank; (B) surface water, Clambank; (C) sediment, Debidue Creek; (D) surface water, Debidue Creek; (E) sediment, Oyster Landing; (F) surface water, Oyster Landing; (G) sediment, Thousand Acre; and (H) surface water, Thousand Acre. Data are shown for biological replicates R1, R2, and R3. Orders representing $<0.5\%$ of relative abundance across all samples were grouped as "Other_Order." **Figure S3:** Relative abundance of Desulfobacteria orders across all sampling dates (June 2020, August 2020, February 2021, and November 2021) in: (A) sediment, Clambank; (B) surface water, Clambank; (C) sediment, Debidue Creek; (D) surface water, Debidue Creek; (E) sediment, Oyster Landing; (F) surface water, Oyster Landing; (G) sediment, Thousand Acre; and (H) surface water, Thousand Acre. Data are shown for biological replicates R1, R2, and R3. Orders representing $<0.5\%$ of relative abundance across all samples were grouped as "Other_Order." **Figure S4:** Potential fungal functional roles and associated taxonomic classes/phyla identified using FUNGuild (Nguyen et al. 2016). Bars represent the number of unique OTUs assigned to each class–function category across (A) sediment and (B) surface water samples from Clambank (CB) and Thousand Acre (TA) marshes in North Inlet–Winyah Bay. **Table S1:** Amplicon analysis pipeline statistics of all samples for 16S reads and were merged by USEARCH v11.0.667. **Table S2:** Results of pairwise PERMANOVA used to compare the 16S prokaryotic communities between sample locations in the North Inlet–Winyah Bay. p-values <0.05 are highlighted in bold font. p-values have been adjusted for multiple comparisons using Benjamini–Hochberg adjustment. **Table S3:** Rarefaction depth for each station and sample type. **Table S4:** Results of PERMANOVA testing the effects of environmental and sampling variables on 16S prokaryotic community composition in the North Inlet–Winyah Bay. p-values <0.05 are shown in bold. R^2 values indicate the proportion of variance explained by each factor. **Table S5:** Taxonomy of identified keystone OTUs ($P_i<0.6$ and $Z_i>1.5$) from the Clambank sediment co-occurrence network. **Table S6:** Taxonomy of bacterial groups with negative and positive connections to fungi in the Clambank sediment network. **Table S7:** Taxonomy of identified keystone OTUs ($P_i<0.6$ and $Z_i>1.5$) from the Clambank surface water co-occurrence network. **Table S8:** Taxonomy of bacterial groups with negative and positive connections to fungi in the Clambank surface water network. **Table S9:** Taxonomy of identified keystone OTUs ($P_i<0.6$ and $Z_i>1.5$) from the Thousand Acre sediment co-occurrence network. **Table S10:** Taxonomy of bacterial groups with negative and positive connections to fungi in the Thousand Acre sediment network. **Table S11:** Taxonomy of identified keystone OTUs ($P_i<0.6$ and $Z_i>1.5$) from the Thousand Acre surface water co-occurrence network. **Table S12:** Taxonomy of bacterial groups with negative and positive connections to fungi in the Thousand Acre surface water network. **Table S13:** Number and percentage of fungal reads mapped to network OTUs by phylum for sediment and surface water samples from Clambank and Thousand Acre in the North Inlet–Winyah Bay. Percentages are calculated from the total fungal reads within each sample type.